11-7-2017

Thermotropic Liquid-crystalline Properties of Extended Viologen Bis(triflimide) Salts

Pradip K. Bhowmik
University of Nevada, Las Vegas, pradip.bhowmik@unlv.edu

Shane T. Killarney
University of Nevada, Las Vegas

Jessa Rose A. Li
University of Nevada, Las Vegas

Jung Jae Koh
University of Nevada, Las Vegas, jung.koh@unlv.edu

Haesook Han
University of Nevada, Las Vegas, haesook.han@unlv.edu

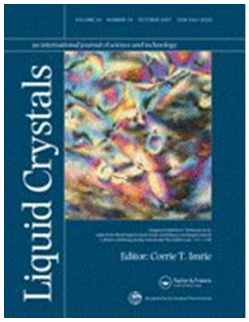

Thermotropic Liquid-Crystalline Properties of Extended Viologen Bis(triflimide) Salts

Journal:	*Liquid Crystals*
Manuscript ID	TLCT-2017-0169.R1
Manuscript Type:	Original Article
Date Submitted by the Author:	23-Sep-2017
Complete List of Authors:	Bhowmik, Pradip; University of Nevada Las Vegas, Chemistry; Killarney, Shane; University of Nevada Las Vegas Li, Jessa; University of Nevada Las Vegas Koh, Jung; University of Nevada Las Vegas, Chemistry and Biochemistry Han, Haesook; University of Nevada Las Vegas, Chemistry Sharpnack, Lewis; Kent State University, Physics Agra-Kooijman, Dena; Kent State University, Physics Fisch, Michael; Kent State University, College of Aeronautics and Engineering Kumar, Satyendra; University at Albany State University of New York
Keywords:	ionic liquid crystals, symmetric viologens, differential scanning calorimetry, polarizing optical microscope, thermotropic, X-ray diffraction, smectic A phase, smectic C phase

Graphical Abstract

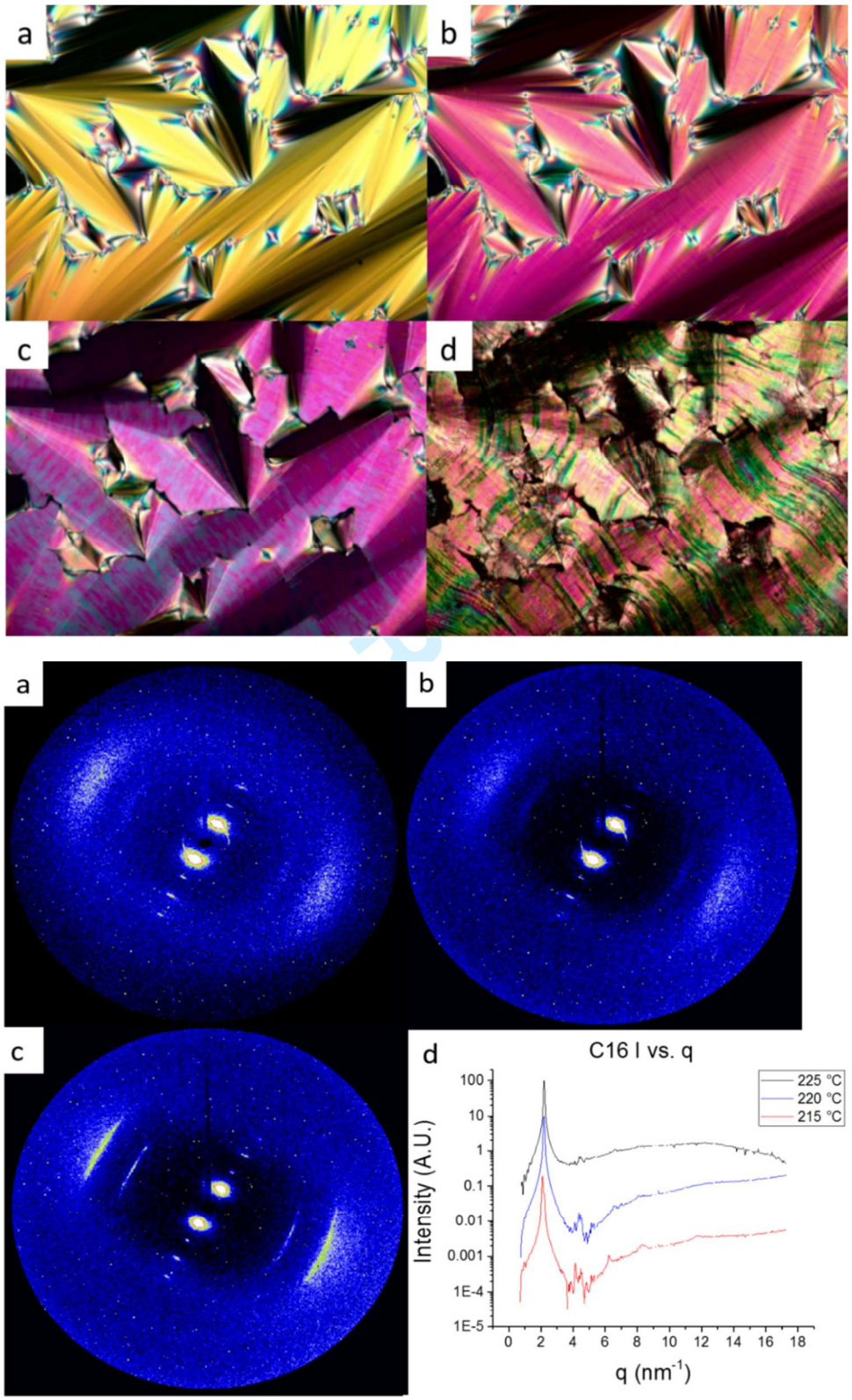

Thermotropic Liquid-Crystalline Properties of Extended Viologen Bis(triflimide) Salts

Pradip K. Bhowmik,[a] Shane T. Killarney,[a] Jessa Rose A. Li,[a] Jung Jae Koh,[a] and Haesook Han[a]
[a]Department of Chemistry and Biochemistry, University of Nevada Las Vegas, 4505 S. Maryland Parkway, Box 454003, Las Vegas, NV 89154, USA
E-mail:pradip.bhowmik@unlv.edu
Lewis Sharpnack[b] Deña M. Agra-Kooijman,[b] Michael R. Fisch,[c] and Satyendra Kumar[d]
[b]Department of Physics and [c]College of Aeronautics and Engineering, Kent State University, Kent, OH 44242, USA
[d]Division of Research, University at Albany, Albany, NY 12222, USA

Abstract

A series of extended, symmetric viologen triflimides were synthesized by the metathesis reaction of lithium triflimide with the respective viologen tosyalates in methanol. Their chemical structures were characterized by Fourier Transform Infrared, ^{1}H and ^{13}C Nuclear Magnetic Resonance spectroscopy and elemental analysis. Their thermotropic liquid-crystalline (LC) properties were examined by a number of experimental techniques including differential scanning calorimetry, thermogravimetric analysis, polarizing optical microscopy and variable temperature X-ray diffraction. The viologen salts containing alkyl chain of two carbon and three carbon atoms were relatively low melting salts. Those of alkyl chains of four carbon and five carbon atoms formed ionic liquids at 88 and 42 °C, respectively. Those of alkyl chain of nine, ten and eleven carbon atoms were high melting salts as high as 166 °C. Those of higher alkyl chains of sixteen, eighteen and twenty carbon atoms showed thermotropic LC phases forming SmC, SmA and an unidentified smectic (Sm) phases, and showed SmA to isotropic transitions at high temperatures. As expected, all the viologen triflimides had excellent stabilities in the temperature range of 338-365 °C.

1. Introduction

The 1,1'-dialkyl-4,4'-bipyridium salts are commonly known as viologens. They are an important class of dicationic compounds and appropriately called functional materials. The multitude of their applications arises because of their redox properties, ionic conductivity, thermochromism, photochromism and electrochromism.[1] Recently, they were studied for the preparation of ever-increasing class of ionic liquids with proper chemical modifications of cations and anions.[2-10] The thermotropic liquid-crystalline (LC) properties of viologens were reported with the variation of several alkyl chain lengths and counterions many years ago by Yu and Samulski.[11] Tabushi et al. also described their thermotropic LC properties of viologen with oligoether linkages and bromide and iodide anions.[12,13] The 1,1'-diphenyl-viologen dialkylbenzenesulfonates with n = 10, 13, and 15 exhibited smectic A (SmA) phases above their melting transitions that persisted up to their decomposition temperatures.[14] Bhowmik et al.[15,16] reported the thermotropic LC properties of a few symmetric viologens (alkyl chains are of equal length) with triflimide ($^{-}NTf_2$) counterions. These salts showed smectic phases at low temperatures and were thermally much more stable than their halide counterparts. They also exhibited LC-to-isotropic transitions without thermal decomposition. They represented some of the most successful examples of halide anion exchange with $^{-}NTf_2$ counterions to lower crystal-to-LC phase transitions. Causin and Saielli [5] studied a series asymmetric viologens (alkyl chains are of unequal length) with this counterion to understand the effect of increasing entropy on the thermotroic LC properties. Strongly asymmetric salts, bearing one short alkyl, do not form LC phases but do form ionic liquids. For other weakly asymmetric salts, they exhibited smectic phases over a broad range of temperatures from 0 to 140 °C. Furthermore, the thermotropic LC properties of symmetric viologen dimers with long alkyl chains and $^{-}NTf_2$ counterions revealed that the linker between viologen moieties enables the formation of a SmA phase in addition highly ordered SmX phase, presumably because it makes the central polycationic region more flexible. Interestingly, the temperature at which the SmX-to-SmA transition takes place is little affected by the length of the outer alkyl substituents. It is presumably dependent on the length of the linker between viologen moieties that remains unexplored to date in the field of ionic liquid crystals (ILCs). Tetracationic salts of this class with short outer substitutents (ethyl group) and various linker lengths do not exhibit thermotropic LC properties.[17,18] Thus, viologens are privileged moieties that are important for the preparation of not only ionic liquids but also ILCs.

The field of ILCs is an active area of research for a decade or so that is manifested in a number of reviews on the topic.[19-24] They have the combined properties of both ionic liquids and liquid crystals. The LC phases offer great advantages over liquid phases. For example, ion conduction is enhanced in the SmA and columnar phases when compared to the isotropic liquid phases. The unique properties of ILCs have widespread applications including display technology, solar cells and ion conductors, templates for the synthesis of nanoparticles. However, they are composed of varied suitably modified cations and anions. Among the common cations are quaternary ammonium, quaternary phosphonium, imidazolium and pyridinium among other cations and the common anions are ^{-}Br, $^{-}NO_3$, $^{-}BF_4$, $^{-}ClO_4$, and $^{-}PF_6$ among other anions. The stable $^{-}NTf_2$ counterion has been extensively used in combination of suitable cations for the preparation of many ionic liquids which have superior physical properties including relatively low viscosities, low melting transitions, high conductivity and high thermal

stability. However, in contrast to the numerous studies of ILs based on $^{-}NTf_2$, [25-27] reports of ILCs on this fluorinated ion are relatively less studied.[5,15,28-32]

As a continuation of our research in the ILC, herein, we describe the synthesis of extended series of symmetric viologen compounds with $^{-}NTf_2$ (n= 2,3,9,10,11,16,18,20; wherein n denotes the carbon atoms in the alkyl chain), characterize their chemical structures by ^{1}H and ^{13}C NMR spectra as well as elemental analysis, and the characterization of their thermotropic LC properties by several experimental techniques including differential scanning calorimetry (DSC), polarizing optical microscopy (POM) and variable temperature X-ray diffraction studies (VT-XRD). Their thermal stabilities by thermogravimeteric analysis (TGA) are also included. The general structures and designations for newly synthesized viologen triflimides as well as previously synthesized viologen triflimides, and their synthetic routes are shown in Scheme 1. The LC properties of this series of symmetric viologen compounds enable one to establish the structure-property relationship of this important class of ILCs and to compare those with the asymmetric viologen compounds.[5] In our previous study, we identified incorrectly LC phases based on the DSC and PLM for the viologen compounds (n = 4,5 and 12) [16] but we corrected these results by VT-XRD studies.

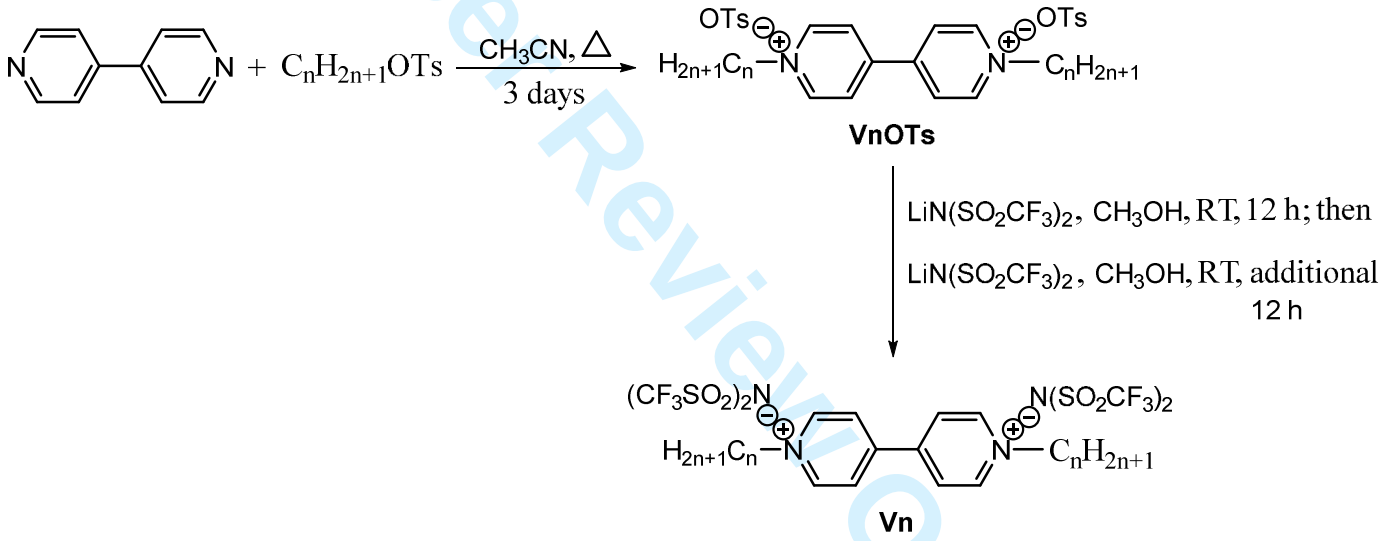

Identification	Yield of metathesis reaction (%)	Previous/Present Study
V1 (n=1)	Quantitative (iodide)	Previous study [16]
V2 (n=2)	52 (tosylate)	Present study
V3 (n=3)	54 (tosylate)	Present study
V4 (n=4)	Quantitative (iodide)	Previous study [16]
V5 (n=5)	Quantitative (bromide)	Previous study [16]
V6 (n=6)	Quantitative (bromide)	Previous study [16]
V7 (n=7)	Quantitative (bromide)	Previous study [15]
V8 (n=8)	Quantitative (bromide)	Previous study [15]
V9 (n=9)	73 (tosylate)	Present study
V10 (n=10)	92 (tosylate)	Present study
V11 (n=11)	96 (tosylate)	Present study
V12 (n=12)	Quantitative (bromide)	Previous study [16]
V14 (n=14)	85 (bromide)	Previous study [17]
V16 (n=16)	82 (tosylate)	Present study
V18 (n=18)	89 (tosylate)	Present study
V20 (n=20)	98 (tosylate)	Present study

Scheme 1. Synthetics routes for the preparation of symmetric viologen triflimides.

2. Experimental Sections

2.1 Instrumentation.

The ^{1}H and ^{13}C nuclear magnetic resonance (NMR) spectra of all of the symmetric viologen salts in CD_3OD were recorded by using VNMR 400 spectrometer operating at 400 and 100 MHz at room temperature. Elemental analysis was performed by Atlanta Microlab Inc., Norcross, GA. Differential scanning calorimetry (DSC) measurements of all of the compounds were conducted on TA module DSC Q200 series in nitrogen at heating and cooling rates of 10 ^{o}C/min. The temperature axis of the DSC thermograms was calibrated before use with reference standards of high purity indium and tin. Their thermogravimetric analyses (TGA) were performed using a TGA Q50 instrument at a heating rate of 10 ºC/min in nitrogen. Optical studies were performed on these viologen salts sandwiched between a standard microscope glass slide and coverslip. The samples were heated and cooled on a Mettler hotstage (FP82HT) and (FP90) controller and observations of the phases made between crossed polarizers of an Olympus BX51 microscope. In short, salts were heated above their clearing transitions and cooled at 5 °C/min to room temperature, with brief pauses to collect images and observe specific transitions. X-ray diffraction studies of salts contained in flame sealed 1 mm quartz capillaries were performed using a Rigaku Screen Machine. The salt under study was placed inside the Linkam HFS350X-Cap capillary hotstage 78 mm away from the 2D detector, with temperature controlled to the accuracy of ± 0.1°C. A magnetic field of ~2.5kG was applied to the samples using a pair of samarium cobalt permanent magnets (with B nearly parallel to the beamstop visible as a vertical in Figures 2 and 5). Scattering patterns were collected using a Mercury 3

CCD detector with resolution 1024×1024 pixels (size: 73.2 μm×73.2 μm) and copper K_α radiation generated by a microfocus sealed X-ray tube with copper anode (λ = 1.542 Å).

2.2 General procedure for the preparation of 4-toluenesulphonates.[33]

4-toluenesulphonyl chloride (27 mmol) was added slowly to a mixture of an aliphatic primary alcohol (25 mmol) and 10 mL of pyridine at 10 °C. The reaction mixture was stirred for 3 h at 20 °C. After that 60 mL of 25% aqueous hydrochloric acid was slowly added. The reaction mixture was then extracted with chloroform, the organic layer dried with Na_2SO_4 and evaporated to yield alkyl 4-toluenesulphonates as colorless oily liquid or white solid, which was used without further purification. The yields of this reaction were comparable to those reported in the literature.[33] The 18- and 20-carbon alkyl tosylates were prepared by following the standard procedure [34] using octadecyl and eicosoyl alcohol, respectively.

2.3 General procedure for the preparation of viologen tosylates.

The symmetrical 1,1'-dialkyl-4,4'-bipyridinium ditosylates were prepared by adding slight excess of two equivalents of n-alkyl tosylate to a solution of one equivalent of 4,4'-bipyridine in acetonitrile on heating to reflux for 3 d. A typical procedure was as follows where the use of n-nonyl tosylate is an example. The requisite amounts of 0.519 g (3.23 mmol) of 4,4'-bipyridine and 2.18 g (7.30 mmol) of nonyl tosylate were dissolved in 25 mL acetonitrile in a single-necked flask on stirring. The contents of reaction flask were heated to reflux for 3 d. The reaction was monitored by thin layer chromatography with the solvents mixture of acetonitrile/water (95/5). After the end of reaction, the contents of the reaction flask was allowed to cool down resulting in the precipitation of product. The precipitate was collected by vacuum filtration. It was then washed with ether and dried at 60 °C in a vacuum oven to give 2.09 g (2.78 mmol) of product. The yield of this tosylate was 84%. Its purity was checked by ^{1}H NMR spectrum and used in the next step for the metathesis reaction. The 20-carbon viologen tosylate was prepared by the identical procedure by using nitromethane that had better solubility of 20-carbon alkyl tosylate than that of usual solvent acetonitrile for quaternization reaction. The yields of viologen tosylates were in the following: 95% for **V2OTs,** 90% for **V3OTs**, 84% for **V9OTs,** 76% for **V10OTs,** 71% for **V11OTs,** 75% for **V16OTs,** 88% for **V18OTs** and 84% for **V20OTs.**

2.4 General procedure for the preparation of viologen triflimides (V2-V3, V9-V11, V16, V18 and V20).

The symmetrical viologen triflimides were prepared by the metathesis reaction of corresponding viologen tosylates with lithium triflimide in a common organic solvent. In a typical procedure, 0.889 g (1.18 mmol) of 1,1'-dinonyl-4,4'-bipyridinium ditosylate was dissolved in 10 mL of methanol in an Erlenmeyer flask. To this solution, 1 mL of methanol solution that contained 0.780 g (2.72 mmol) of lithium triflimide was slowly added on stirring at room temperature. The stirring was continued for 12 h. After the end of this time period, methanol was removed in a rotary evaporator, water was added to the crude products to dissolve lithium tosylate and excess lithium triflimide, thus giving the desired compound. To check the completion of metathesis reaction, the analysis of ^{1}H NMR spectrum was used. If not, the metathesis reaction was repeated one more time by using a fresh amount (0.780 g, 2.72 mmol) of lithium triflimide and stirring for an additional 12 h period. The workup procedure was repeated for all of the salts in the series. The typical yields of viologen triflimides for the metathesis reaction were in the range of 85-90% with a few exceptions. For example, the yield of viologen triflimide (**V9**) was (0.800 g, 0.86 mmol) 73%.

Typical data for **V2:** Yield 52%. δ_H (CD_3OD, 400 MHz, ppm): 9.22-9.23 (4H, d, J = 6.8 Hz), 8.60-8.61 (4H, d, J = 5.6 Hz), 4.75-4.79 (4H, q, J = 14.8 Hz), 1.70-1.74 (6H, t, J = 14.8 Hz). δ_C (CD_3OD, 400 MHz, ppm): 150.02, 145.39, 126.92, 124.51, 121.31, 118.12, 116.43, 57.38, 15.22. Anal. calcd for $C_{18}H_{18}N_4O_8F_{12}S_4$ (774.61): C, 27.90; H, 2.34; N, 7.23; S, 16.56. Found C, 27.94; H, 2.34; N, 7.32; S, 16.33.

Data for **V3:** Yield 54%. δ_H (CD_3OD, 400 MHz, ppm): 9.22-9.24 (4H, d, J = 6.8 Hz), 8.62-8.64 (4H, d, J = 6.4 Hz), 4.68-4.72 (4H, t, J = 14.8 Hz), 2.15 (4H, m) 1.05-1.08 (6H, t, J = 14.8 Hz). δ_C (CD_3OD, 400 MHz, ppm): 151.53, 147.10, 128.37, 125.99, 122.80, 119.62, 116.43, 64.71, 25.92, 10.75. Anal. calcd for $C_{20}H_{22}N_4O_8F_{12}S_4$ (802.66): C, 29.93; H, 2.76; N, 6.98; S, 15.98. Found C, 29.93; H, 2.62; N, 7.12; S, 16.12.

Data for **V9:** δ_H (CD_3OD, 400 MHz, ppm): 9.23-9.25 (4H, d, J = 6.8 Hz), 8.62-8.64 (4H, d, J = 6.4 Hz), 4.71-4.75 (4H, t, J = 14.8 Hz), 2.08 (4H, m), 1.29-1.43 (24H, m) 0.88-0.92 (6H, t, J = 14.8 Hz). δ_C (CD_3OD, 400 MHz, ppm): 151.48, 147.08, 128.36, 125.99, 122.80, 119.62, 116.43, 63.42, 33.01, 32.60, 30.47, 30.34, 30.16, 27.24, 23.73, 14.44. Anal. calcd for $C_{32}H_{46}N_4O_8F_{12}S_4$ (970.97): C, 39.58; H, 4.78; N, 5.77; S, 13.21. Found C, 39.40; H, 4.73; N, 5.77.12; S, 13.37.

Data for **V10:** Yield 92%. δ_H (CD_3OD, 400 MHz, ppm): 9.22-9.24 (4H, d, J = 6.8 Hz), 8.61-8.63 (4H, d, J = 6.4 Hz), 4.71-4.75 (4H, t, J = 15.2 Hz), 2.08 (4H, m), 1.29-1.42 (28H, m) 0.87-0.91 (6H, t, J = 14.0 Hz). δ_C (CD_3OD, 400 MHz, ppm): 151.48, 147.08, 128.36, 125.99, 122.81, 119.62, 116.43, 63.43, 33.06, 32.60, 30.63, 30.51, 30.43, 30.16, 27.25, 23.75, 14.45. Anal. calcd for $C_{34}H_{50}N_4O_8F_{12}S_4$ (999.02): C, 40.88; H, 5.04; N, 5.61; S, 12.84. Found C, 40.34; H, 5.06; N, 5.44; S, 12.88.

Data for **V11:** Yield 96%. δ_H (CD_3OD, 400 MHz, ppm): 9.22-9.24 (4H, d, J = 6.8 Hz), 8.61-8.63 (4H, d, J = 6.4 Hz), 4.70-4.74 (4H, t, J = 15.2 Hz), 2.08 (4H, m), 1.29-1.42 (32H, m) 0.87-0.91 (6H, t, J = 14.0 Hz). δ_C (CD_3OD, 400 MHz, ppm): 151.48, 147.08, 128.36, 125.99, 122.81, 119.62, 116.43, 63.42, 33.09, 32.60, 30.72, 30.67, 30.51, 30.47, 30.16, 27.25, 23.76, 14.45. Anal. calcd for $C_{36}H_{54}N_4O_8F_{12}S_4$ (1027.08): C, 42.10; H, 5.30; N, 5.45; S, 12.49. Found C, 41.82; H, 5.16; N, 5.33; S, 12.65.

Data for **V16:** Yield 82%. δ_H (CD_3OD, 400 MHz, ppm): 9.22-9.24 (4H, d, J = 6.8 Hz), 8.61-8.63 (4H, d, J = 6.4 Hz), 4.70-4.74 (4H, t, J = 15.2 Hz), 2.05-2.10 (4H, m), 1.28-1.42 (52H, m) 0.88-0.91 (6H, t, J = 14.0 Hz). δ_C (CD_3OD, 400 MHz, ppm): 151.46, 147.07, 128.35, 125.99, 122.78, 119.61, 116.43, 63.42, 33.11, 32.60, 30.82, 30.81, 30.79, 30.75, 30.67, 30.51, 30.50, 30.17, 27.25, 23.76, 14.47. Anal. calcd for $C_{46}H_{74}N_4O_8F_{12}S_4$ (1167.30): C, 47.33; H, 6.39; N, 4.80; S, 10.99. Found C, 47.59; H, 6.42; N, 4.83; S, 11.14.

Data for **V18:** Yield 89%. δ_H (CD_3OD, 400 MHz, ppm): 9.23-9.25 (4H, d, J = 7.2 Hz), 8.62-8.64 (4H, d, J = 6.8 Hz), 4.71-4.74 (4H, t, J = 15.2 Hz), 2.05-2.10 (4H, m), 1.23-1.42 (60H, m) 0.88-0.91 (6H, t, J = 14.0 Hz). δ_C (CD_3OD, 400 MHz, ppm): 151.47, 147.08, 128.35, 125.99 (weak), 122.81, 119.62, 116.43 (weak), 63.42, 33.12, 32.61, 30.82, 30.80, 30.76, 30.67, 30.52,

30.51, 30.18, 27.25, 23.77, 14.48. Anal. calcd for $C_{50}H_{82}N_4O_8F_{12}S_4$ (1222.50): C, 49.09; H, 6.76; N, 4.58; S, 10.48. Found C, 49.13; H, 6.71; N, 4.53; S, 11.01.

Data for **V20:** Yield 98%. δ_H (CD_3OD, 400 MHz, ppm): 9.34-9.35 (4H, d, J = 6.8 Hz), 8.62-8.64 (4H, d, J = 6.8 Hz), 4.65 (4H, t, J = 15.2 Hz), 1.94-1.96 (4H, m), 1.20-1.28 (68H, m) 0.80-0.83 (6H, t, J = 13.6 Hz). δ_C (CD_3OD, 400 MHz, ppm): 149.03, 146.16, 127.00, 125.99 (weak), 121.49, 118.29, 116.43 (weak), 61.40, 31.73, 31.17, 29.46, 29.38, 29.25, 29.14, 28.86, 25.86, 22.52, 14.33. Anal. calcd for $C_{54}H_{90}N_4O_8F_{12}S_4$ (1279.56): C, 50.69; H, 7.09; N, 4.38; S, 10.02. Found C, 50.93; H, 7.16; N, 4.40; S, 9.92.

3. Results and discussion

3.1 Synthesis of viologen triflimides

All of these viologen triflimides (**V2, V3, V9, V10, V11, V12, V16, V18** and **V20**) were prepared from the corresponding viologen tosylates by the metathesis reaction in methanol with high purity and high yields. The viologen tosylates were prepared by the quaternization reaction of 4,4'-bipyridyl with the corresponding alkyl tosylates in acetonitrile. The quaternization reaction with 20-cabon alkyl tosylate was carried out in nitromethane instead of the usual solvent acetonitrile.

3.2 Thermal properties, variable temperature XRD and optical textures.[35-39]

V2 exhibited a single endotherm and a single exotherm in the first heating and first cooling cycles, respectively. Similarly, it showed single endotherm and exotherm in the second heating and second cooling cycles, respectively. In conjunction with POM, this endotherm corresponded to the crystal → liquid transition, T_m, at 136 °C with ΔH = 50.1 J/g (not shown). The cooling exotherm was related to the liquid-crystal transition, T_c, with the identical heat of enthalpy; and it showed appreciate degree of supercooling. Thus, it was found that it had not only slightly higher T_m but also higher heat of enthalpy than those of **V1.**[16]

V3 showed a single endotherm and a single exotherm in the first heating and first cooling cycles, respectively. Similarly, it showed single endotherm and exotherm in the second heating and second cooling cycles, respectively. In conjunction with POM, this endotherm corresponded to the crystal → liquid transition, T_m, at 106 °C with ΔH = 65.8 J/g (not shown). The cooling exotherm was related to the liquid-crystal transition, T_c, with the identical heat of enthalpy; and it underwent appreciate degree of supercooling. It had lower T_m than that of either **V1** or **V2,** but higher heat of enthalpy than that of either **V1** or **V2.** Therefore, **V1-V3** are high melting salts (melting transtions >100 °C).

In the previous study for **V4** and **V5,** we identified erroneously their LC phases based on DSC and POM, but in conjunction with VT-XRD studies we found that both of these viologen salts were of ionic liquids not ILCs. They exhibited two endotherms in their DSC thermograms: one at low-temperature and the other at high-temperature. The high-temperature endotherms at 88 and 42 °C were their crystal-melting transitions, respectively. The low-temperature endotherms were related to crystal-crystal transitions at 51 and -4 °C, respectively, since they exhibited crystalline diffraction patterns (not shown) after their first endothermic peaks. Therefore, it was found that **V4** and **V5** are the ionic liquids and **V5** has the lowest meting

transition at 42 °C. In the previous studies, we reported that **V6, V7,** and **V8** showed crystal-LC transitions, T_m values, at 58, 41, and 37 °C and LC-liquid transitions, T_i values, at 78, 112, and 136 °C, respectively. They showed SmA phase and relatively a wide range of LC phase of 20, 71, and 99 °C, respectively. In fact, these are first examples of viologen salts containing triflimides as counterions that exhibit SmA phase.

V9 showed two endotherms in the first heating cycle and two exotherms in the first cooling cycle. Similarly, it also showed two endotherms and exotherms in the second heating and cooling cycles, respectively. The low-temperature endotherm had a higher heat of enthalpy than that of the high-temperature endotherm in both the heating cycles. In conjunction with VT-XRD studies, it was found that low-temperature endotherm was related to crystal-crystal transition, since its diffraction pattern taken at 23 °C showed sharp rings suggestive of its polycrystalline nature. The high-temperature endotherm was related to crystal-liquid transition, since it showed diffuse rings at 150 °C. Thus, it did not show any LC phase as opposed to **V6, V7** and **V8.**

Like **V9, V10** also showed two endotherms in the first heating and two exotherms in the first cooling cycle. Similarly, it also showed two endotherms and exotherms in the second heating and cooling cycles, respectively. The low-temperature endotherm had much higher heat of enthalpy than that of high-temperature endotherm in both the heating cycles. In conjunction with VT-XRD studies, it was confirmed that low-temperature endotherm was related to crystal-crystal transition, since its diffraction pattern taken at 120 °C showed sharp rings suggestive of its polycrystalline nature. The high-temperature endotherm was related to crystal-liquid transition, since it showed diffuse rings at 180 °C. Thus, it also did not show an LC phase as opposed to **V6, V7** and **V8.**

Like **V9** and **V10**, **V11** also showed two endotherms in the first heating and two exotherms in the first cooling cycle. Similarly, it also showed two endotherms and exotherms in the second heating and cooling cycles, respectively. The low-temperature endotherm had much higher heat of enthalpy than that of high-temperature endotherm in both the heating cycles. In conjunction with VT-XRD studies, it was confirmed that low-temperature endotherm was related to crystal-crystal transition, since its diffraction pattern taken at 140 °C showed several sharp rings in the wide angle region suggestive of its multidomain structure with some large crystallites. The high-temperature endotherm was related to crystal-liquid transition, since it showed diffuse rings at 200 °C. Thus, it also did not show any LC phase as opposed to **V6, V7** and **V8.** The typical DSC thermograms of **V11** as representatives of **V9-V11** are shown in Figure 1.

In our previous study for **V12,** we identified erroneously their LC phases based on DSC and PLM, but in conjunction with VT-XRD studies we found in the present study that this high melting temperature viologen salt does not form an LC phase. It showed multiple endotherms in its DSC thermograms and its lowest temperature endotherm had the highest heat of enthalpy than those of other transitions, like **V9, V10** and **V11.** The low-temperature endotherms were all related to

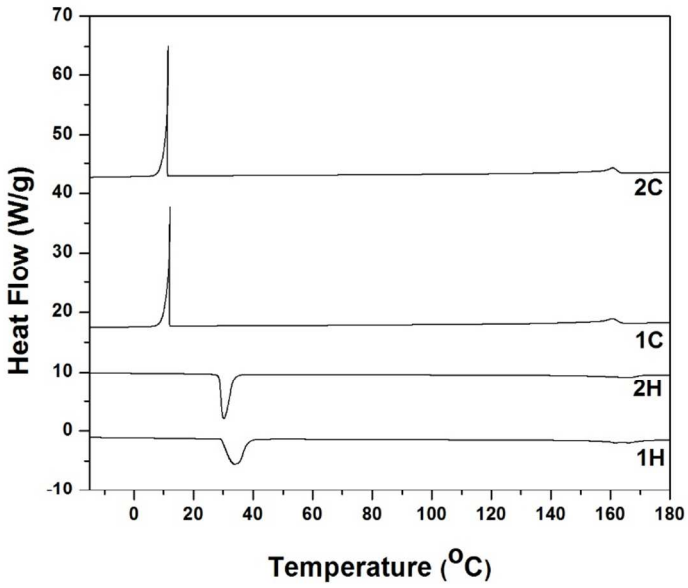

Figure 1. DSC thermograms of **V11** obtained at heating and cooling rates of 10 °C/min in nitrogen.

crystal-crystal transitions, since a diffraction pattern taken at 60 °C showed sharp rings indicating its polycrystalline nature. The highest-temperature endotherm was related to the crystal → liquid transition, since its diffraction pattern taken at 200 °C showed diffuse rings that are typical of isotropic liquid phase. Therefore it was found that, like **V9, V10,** and **V11**, it did not form any LC phase that are in contrast to **V6, V7** and **V8.** The X-ray diffraction patterns in the crystalline and isotropic phase of **V9-V12** are shown in Figure 2.

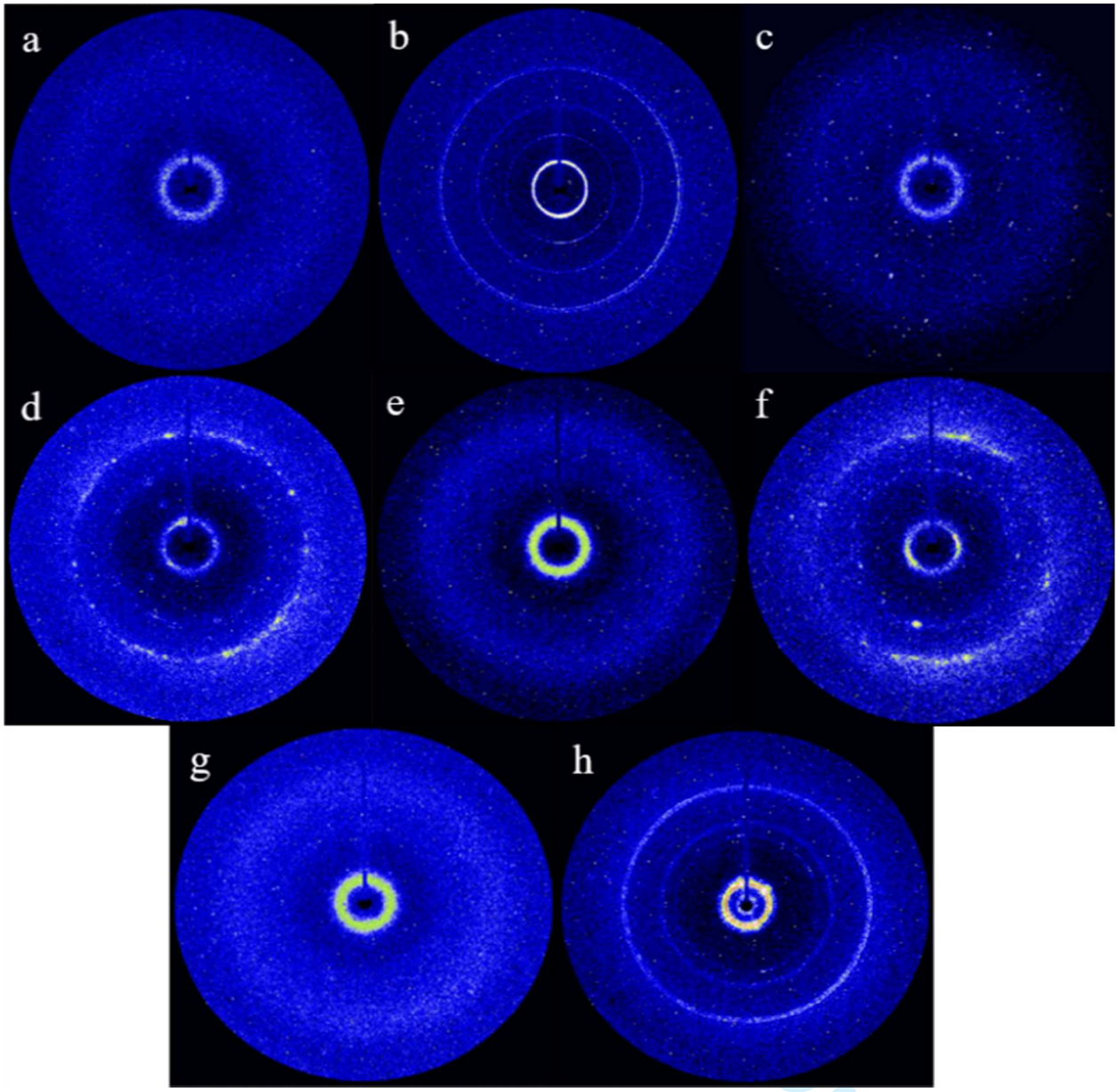

Figure 2. The x-ray diffraction patterns of **V9, V10, C11,** and **V12.** a) Isotropic **V9** at 150 °C, showing diffuse scattering rings. b) Crystalline **V9** at 23 °C with sharp rings indicating a polycrystalline sample. c) Isotropic **V10** at 180 °C, showing diffuse scattering rings. d) Crystalline **V10** at 120 °C, showing several sharp peaks in the wide angle region indicating a multidomain sample with some large crystallites. e) Isotropic **V11** at 200 °C, showing diffuse scattering rings. f) Crystalline **V11** at 140 °C showing, showing several sharp peaks in the wide angle region indicating a multidomain sample with some large crystallites. g) Isotropic **V12** at 200 °C, showing diffuse scattering rings. h) Crystalline **V12** at 60 °C showing sharp rings indicating a polycrystalline sample.

While this present study is in progress, Casella et al. [17] reported the results of **V14** that exhibited two major endotherms in DSC thermograms in first and second heating cycles. It also showed two exotherms in the cooling cycles. After extensive studies with POM, VT-XRD and solid-state ^{1}H-^{13}C CP-MAS and ^{19}F NMR spectroscopy suggested that low-temperature endothem at 42 °C was related to crystal-SmX transition wherein alkyl chains were almost entirely a molten phase, but that there existed a high degree of order within the ionic sublayers. The observation of striated focal conic texture and mosaic textures was consistent with a high ordered SmX phase. The high-temperature endotherm at 218 °C corresponded to SmX phase to isotropic liquid phase, which was in sharp contrast to **V9-V12.** We also synthesized and characterized **V14** that were consistent with the results as reported by Casella et al.[17]

The DSC thermograms of **V16** obtained at heating and cooling rates 10 °C/min in nitrogen are shown in Figure 3. Unlike **V14,** it showed distinctly three endotherms in the heating cycles and three exotherms in the cooling cycles. Figure 4a shows the optical textures observed in **V16** at 216 °C. The textures reveal a typical focal conic texture, characteristic of the SmA phase, which begins to appear at 233 °C. This phase is confirmed in the x-ray diffraction pattern at

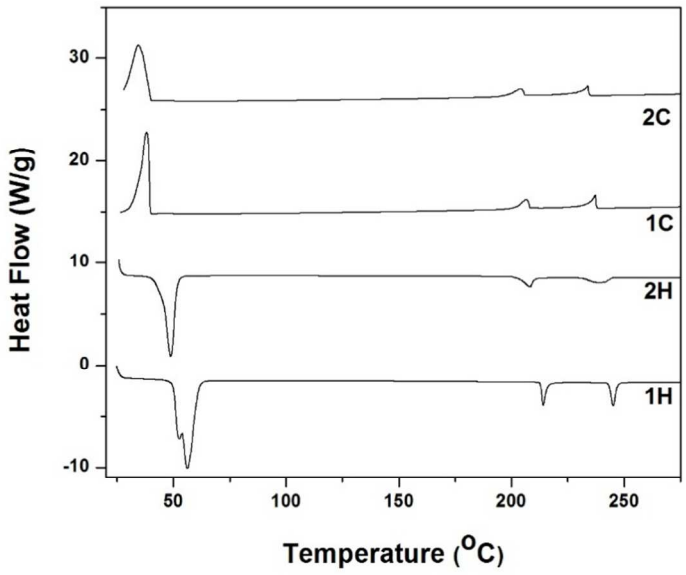

Figure 3. DSC thermograms of **V16** obtained at heating and cooling rates of 10 °C/min in nitrogen.

225 °C, shown in Figure 5a. The wide angle scattering shows two diffuse arcs, centered at 4.9 Å, indicating alignment but no long range positional order of the molecule within the smectic layers. The small and wide angle scattering peaks are oriented at 90 degrees from each other, indicating that the molecules are oriented orthogonally to the smectic layers, with a layer spacing of 28.6 Å in a SmA phase. This spacing is about $0.50L_{C16}$, where L_{C16} is the estimated molecular length, 46.9 Å of the molecule. Upon further cooling the focal conic domains begin to break up, with thin lines crossing the domains as shown optically in Figure 4b. These lines indicate a transition to higher order smectic phase, which x-ray diffraction data indicate is the SmC phase.

This is shown in Figure 5b, the scattering pattern observed at 220 °C, with a smectic layer spacing of 28.2 Å. Additional cooling causes significant breakup of the focal conics and at 151°C, the sample transitions into an unknown higher order phase, as shown in Figure 4c. The X-ray diffraction pattern at wide angle becomes sharp, with peaks at 7.5 and 4.9 Å, indicating in-plane order of the molecules within the smectic layers (Figure 5c). Determination of the exact smectic phase requires an experimental set-up with scattering plane parallel to the smectic layers which is not possible for the sample geometry. The smectic layer spacing calculated from the small angle peaks in this phase is 30.1 Å. Thus, the three endotherms in DSC thermograms corresponded to crystal to SmC, SmC to SmA and SmA to isotropic liquid phase transition.

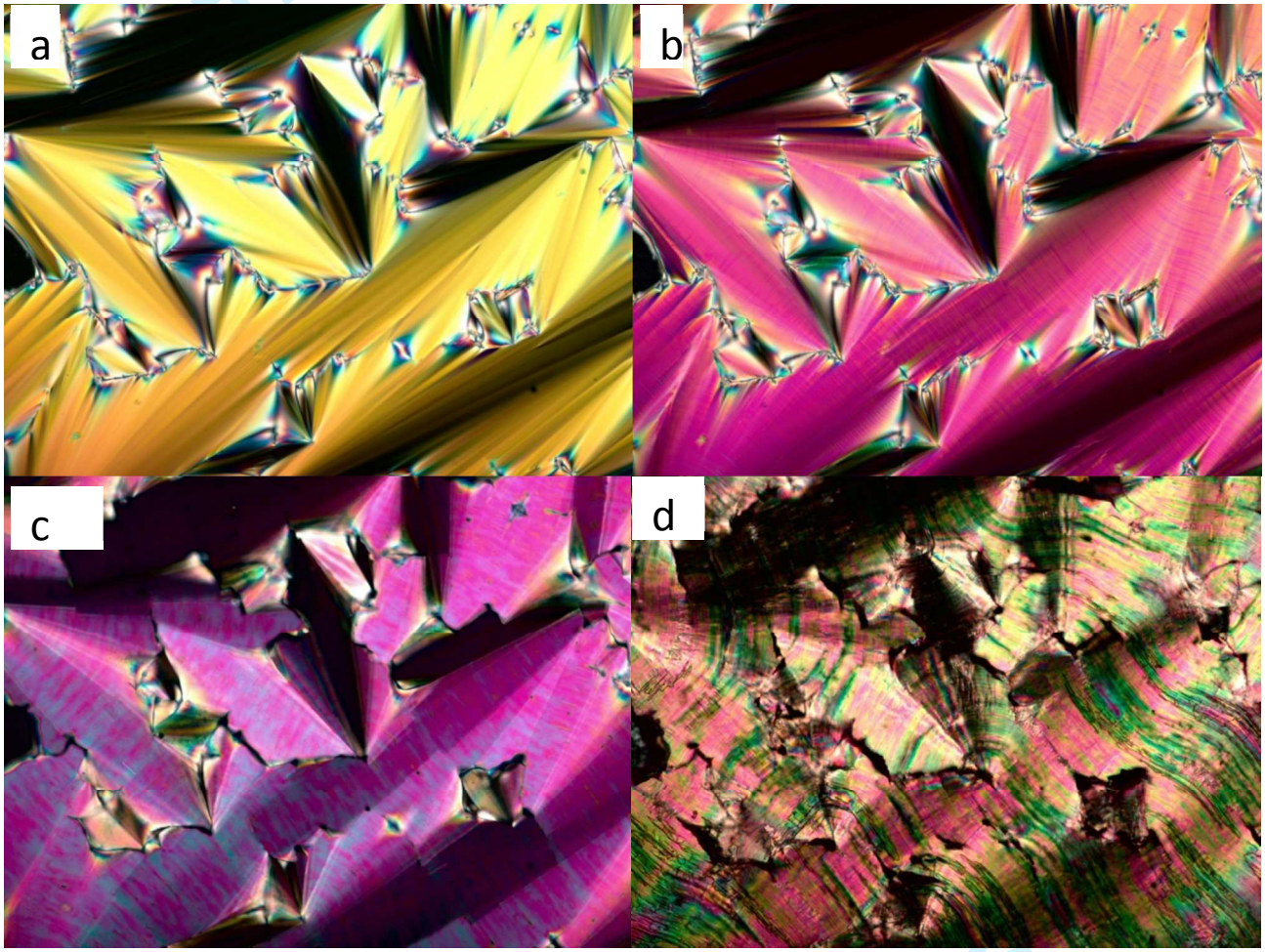

Figure 4. The optical textures of **V16** observed upon cooling a fresh sample at 5°C/min in a hotstage between crossed polarizers at 200x magnification. a) The focal conic texture of the SmA phase observed at 216 °C. b) The SmC phase observed at 191 °C upon further cooling from the SmA phase. Note that the appearance of lines running across the focal conic domain. c) At 151°C SmX phase observed upon further cooling from the SmC phase. Although there are temperature mismatches between the transition temperatures observed from XRD and optical studies, it does appear that this salt possesses a higher order smectic phase below the C phase, however, poor alignment and low scattering intensity makes determination of the nature of this

phase impossible with the techniques employed in this study. d) The crystalline phase of **V16** at 41 °C.

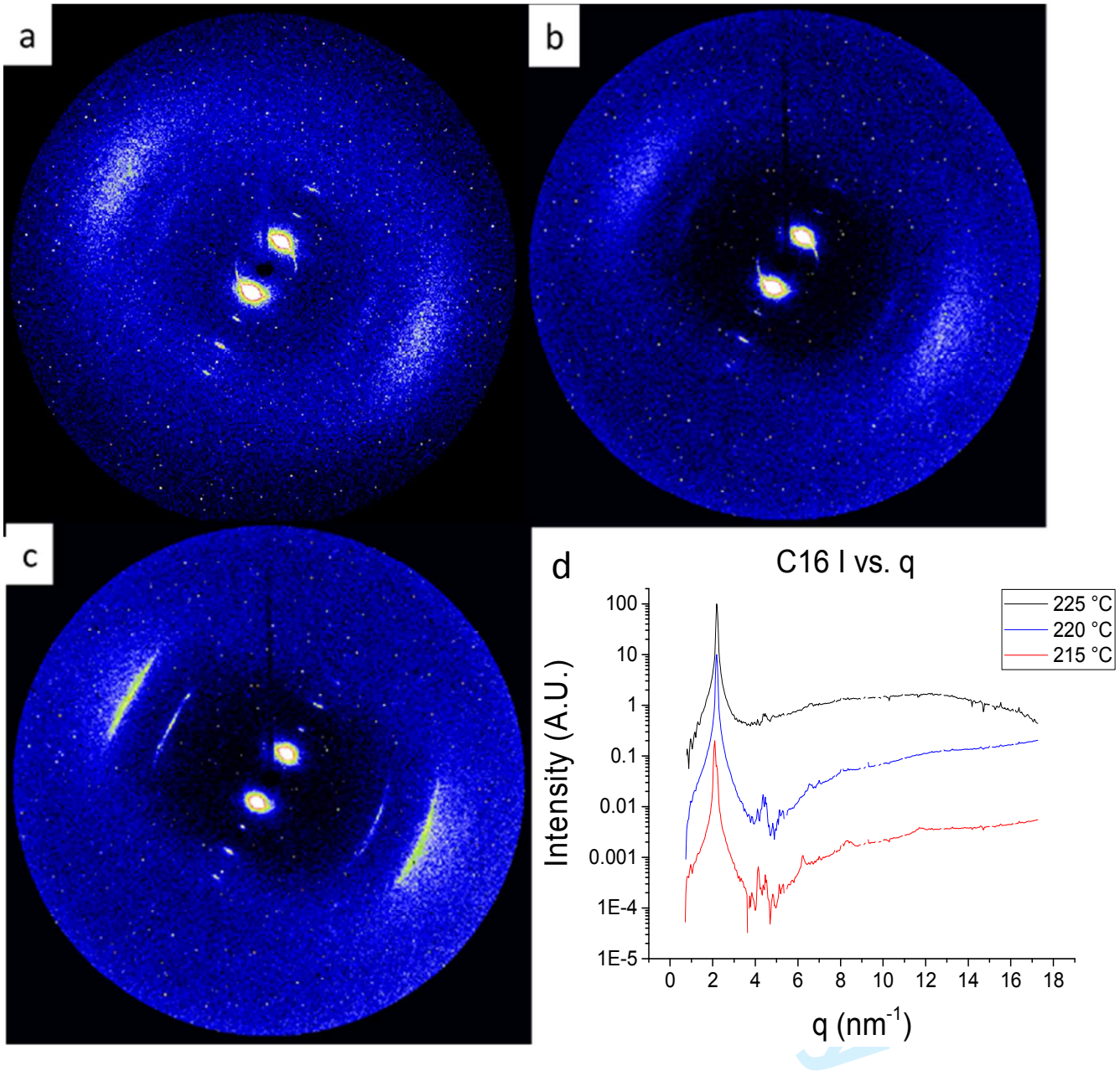

Figure 5. The x-ray diffraction patterns of **V16,** cooled at 0.5°C/min. a) The diffraction pattern produced by **V16** in the SmA phase at 225 °C. b) The pattern observed at 220 °C, showing sharp inner and diffuse outer arcs. The rotation of the inner arcs with respect to the outer arcs indicates molecular tilt relative to the smectic planes, indicating the SmC phase. c) The sharp outer peaks of **V16** at 215 °C indicate the presence of a higher order structure. It could be the result of slow crystallization or a transition into a higher order smectic phase. (d) I vs q shown for the XRD patterns in Figures 5a-c.

The DSC thermograms of **V18** obtained at heating and cooling rates 10 °C/min in nitrogen are shown in Figure 6. Like **V14,** it showed distinctly two endotherms in the heating cycles and two exotherms in the cooling cycles, respectively. Starting with the optical textures for the salt

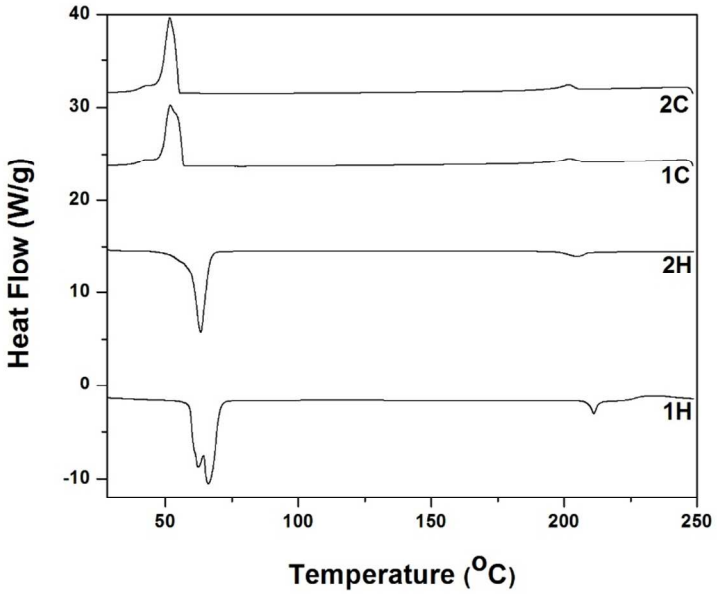

Figure 6. DSC thermograms of **V18** obtained at heating and cooling rates of 10 °C/min in nitrogen.

V18 shown in Figure 7a, we clearly see the focal conic texture of the SmA phase formed upon cooling from the isotropic state at 184 °C. The x-ray diffraction pattern shown in Figure 8a shows the expected sharp small angle arcs expected in the SmA phase. The corresponding smectic layer spacing is 30.0 Å. The spacing is approximately $0.58L_{C18}$, where L_{C18} = 52.0 Å is the calculated molecular length (Avogadro®).[40] We note that the wide angle arcs, centered at 4.6 Å, are very broad and attribute this to the disorder of the hydrocarbon tails. The focal conic domain begins to break up at 171 °C showing lines forming across the domain, indicating a transition to the SmC phase, shown in Figure 8b. This phase was neither observed in the x-ray data nor in the DSC thermograms. The temperature range of SmC phase in the salt prepared in capillaries was too narrow for observation, which we attribute to the volatilization of this salt from the LC phase. Additional cooling causes the focal conic domains to break apart as shown in Figure 8c. This phase still shows the sharp inner arcs, centered at 30.2 Å, of a smectic phase, Figure 8b, but the wide angle peaks, centered at 7.6 and 5.3 Å, are too sharp to be either the SmA or SmC phase. We were not able to determine the exact phase present from XRD, so we label this higher order smectic phase as SmX. Upon cooling to near room temperature, the sample crystallizes. Optically, this transition occurred at 54 °C. In the X-ray data, this salt began to

crystallize at 45 °C, however, the image shown in Figure 8c is at 23°C, to better show the ring pattern of the crystal.

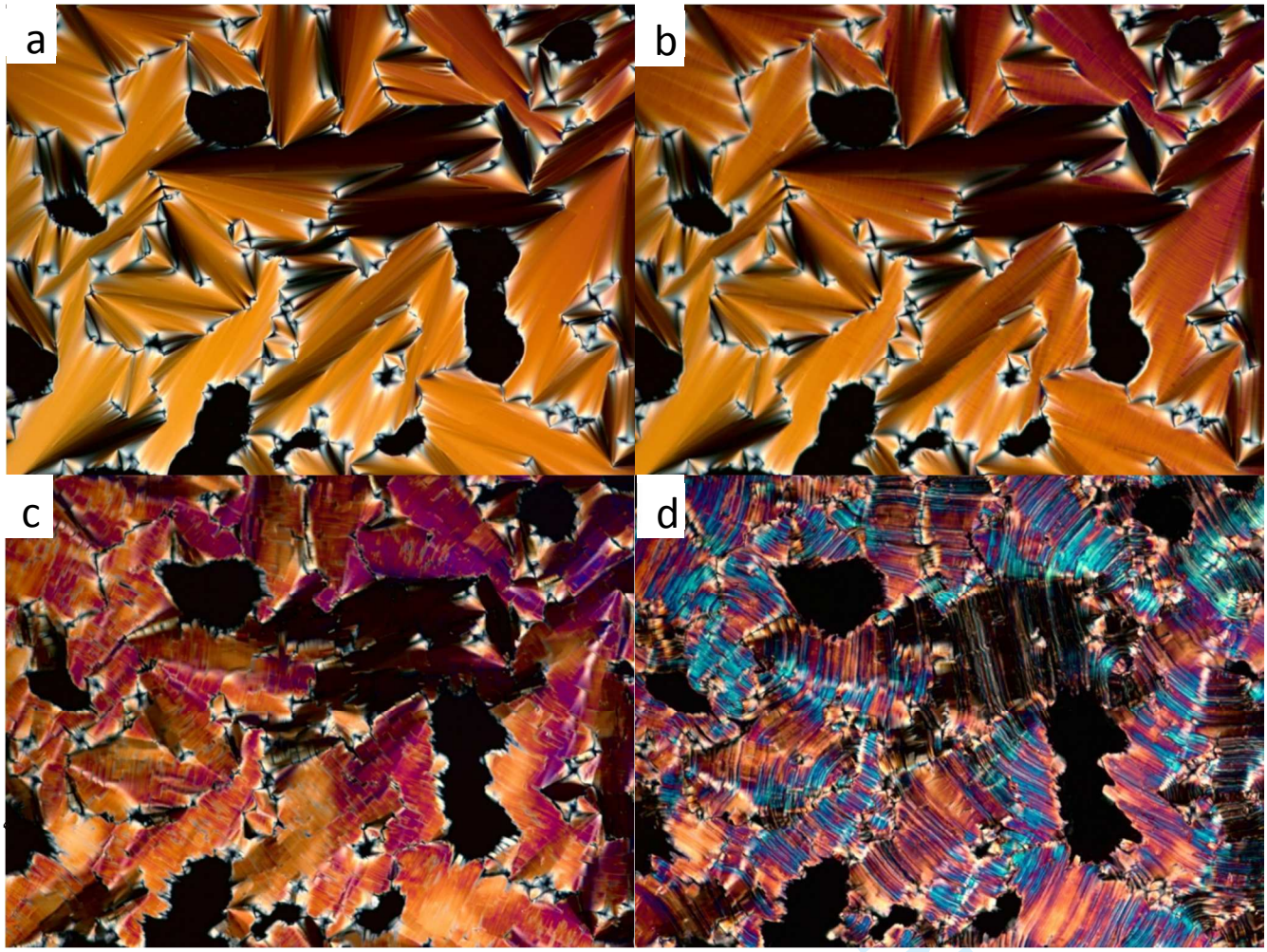

Figure 7. The optical textures observed in **V18** when cooled from above the clearing point at 5 °C/min. a) The focal conic texture of **V18** at 184 °C. b) The focal conic texture begins to break up at 171 °C showing lines across the focal conic domains, indicating a transition to the SmC phase. c) The texture of the unknown SmX phase at 113 °C. d) The texture of the crystalline phase of **V18.**

The temperature discrepancies between the phases observed with XRD, optically and even DSC thermograms and repeated heating and cooling may result from the volatilization of these salts (**V16** and **V18**) at high temperatures. In particular, the salts produced bubble when heated to their clearing temperatures in the quartz capillaries during the preparation of samples. After extensive degassing at 100 °C under vacuum, we ruled out organic solvents remaining in

the salts during synthesis. Note here that, the volatility of pyridinium and imidazolium ion liquids containing triflimide ions has been well documented in the literature.[41-44]

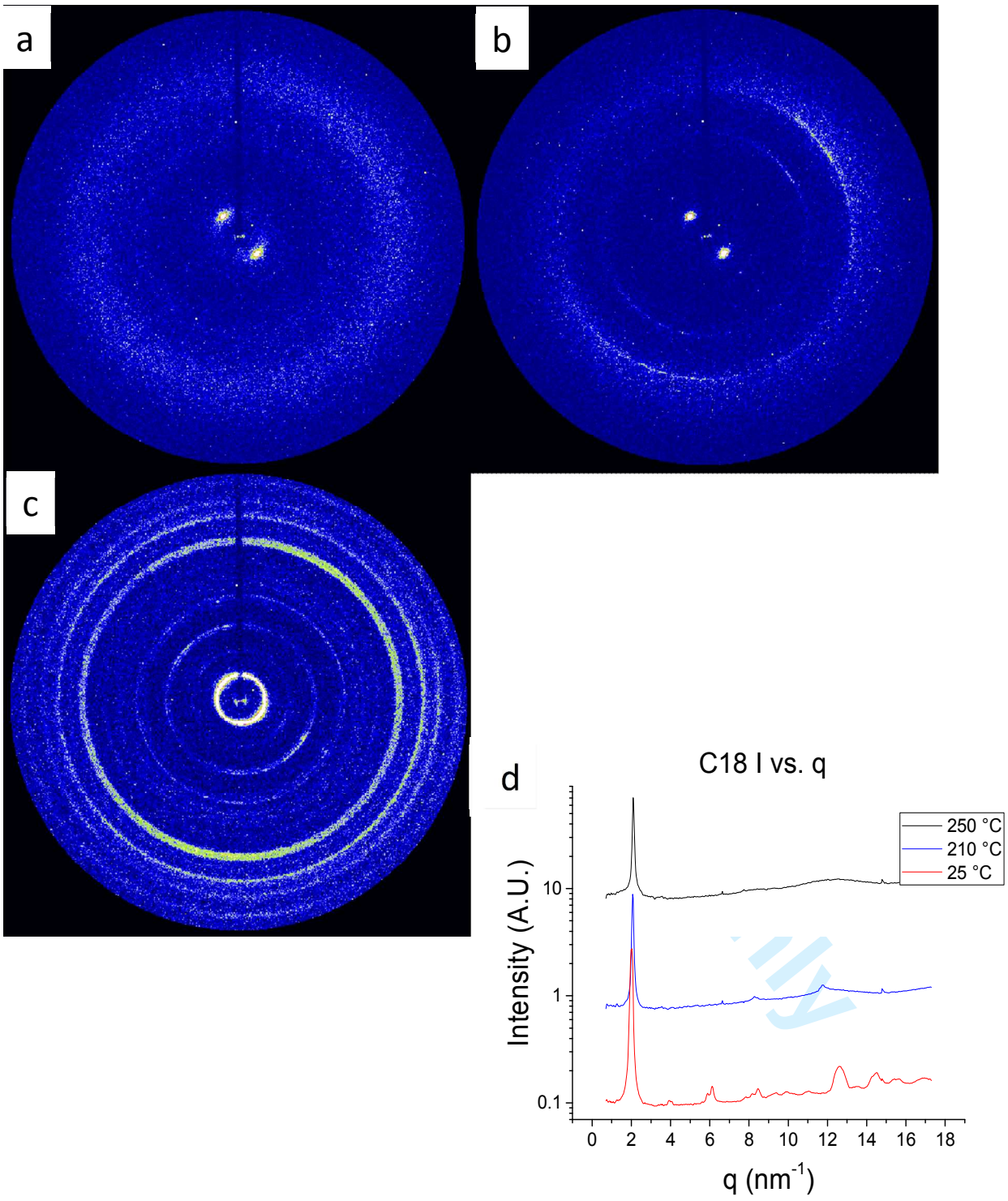

Figure 8. X-ray diffraction patterns of **V18** cooled at 0.5°C/min. a) The SmA showing sharp inner arcs observed at 250 °C. b) Higher order smectic X phase observed at 210 °C. Note the

sharp outer peaks in addition to the sharp inner arc. c) The diffraction pattern of crystalline **V18** observed at 25 °C, showing many sharp rings indicating randomly oriented small domains. (d) I vs q shown for the XRD patterns in Figures 8a-c.

The DSC thermograms of **V20** obtained at heating and cooling rates 10 °C/min in nitrogen are shown in Figure S12. It contained four endotherms in the first heating and the second heating cycles, but three exotherms in the first cooling and second cooling cycles. POM studies suggested that this salt had the similar optical texture as observed in **V16.** The lowest temperature endotherm (61 °C) was related to the crystal-crystal transition that was followed by crystal-SmC (72 °C). The other two high-temperature endotherms presumably were related to SmC-SmA (210 °C) and SmA–isotropic transition (288 °C), respectively.

The thermodynamic properties of phase transition temperatures of symmetric viologen triflimides from DSC measurements and comments on POM and VT-XRD studies are given in Table 1

Table 1. Thermodynamic properties of phase transition temperatures of symmetric viologen triflimide obtained from DSC measurements and comments on POM and VT-XRD studies. Phase transition temperatures (°C) and their enthalpy changes (kJ/mol) taken from the first heating cycle.

Identification	Phase Transition Temperature	Comments on POM and VT-XRD
V1	Cr 132 (39.0) I	Not LC Previous study [16]
V2	Cr 136 (38.2) I	Not LC Present study
V3	Cr 106 (53.0) I	Not LC Present study
V4	Cr 51 (14.7) Cr 88 (27.6) I	Not LC Previous study* 16]
V5	Cr -4.3 (3.9) Cr 42 (19.0) I	Not LC Previous study* [16]
V6	Cr 58 (31.0) SmA 78 (5.0) I	LC Previous study [16]
V7	Cr 41 (14.4) SmA 112 (8.7) I	LC Previous study [15]
V8	Cr 37 (33.4) SmA 136 (9.3) I	LC Previous study [15]
V9	Cr 22 (18.8) Cr 154 (11.4) I	Not LC Present study
V10	Cr 39 (27.4) Cr 150 (4.9) I	Not LC Present study
V11	Cr 34 (27.7) Cr 166 (4.6) I	Not LC Present study
V12	Cr 28 (27.2) Cr 120 (8.0) Cr 199 (9.9) I	Not LC Previous study* [16]
V14	Cr 42 (49.1) SmX 218 (15.2) I	LC Previous study [17]
V16	Cr 56 (78.1) SmC 214 (5.8) SmA 245 (6.7) I	LC Present study
V18	Cr 66 (92.1) SmA 211 (4.8) I	LC Present study
V20	Cr 61(20.6) Cr 72 (64.1) SmC 210 (5.1) SmA 288 (4.8) I	LC Present study

Cr-Crystal, I-Isotropic, SmA-Smectic A, SmC-Smectic C and SmX-Unidentified smectic phase. *Corrected.

3.3 Thermal stabilities of symmetric viologen triflimides

The stabilities for all of viologen were studied by TGA analyses and are defined as the temperature (°C) at which a 5% weight loss for each of the salts occurred at a heating rate of 10 °C/min in nitrogen. Despite the presence of flexible alkyl chains, TGA thermograms of these

salts as shown in Figure 9 show relatively high thermal stabilities that are in the temperature range of 338-365 °C. These temperatures gradually decrease slightly with the increase in carbon number in the alkyl chain. Triflimide is one of best counterion that impart the high thermal stability of ionic liquids and ionic polymers reported in the literature,[45-47] because it has non-nucleophilic character being the conjugate base of a super acid. Therefore, it decomposes the cationic moieties nuclophilically at relatively high temperatures.

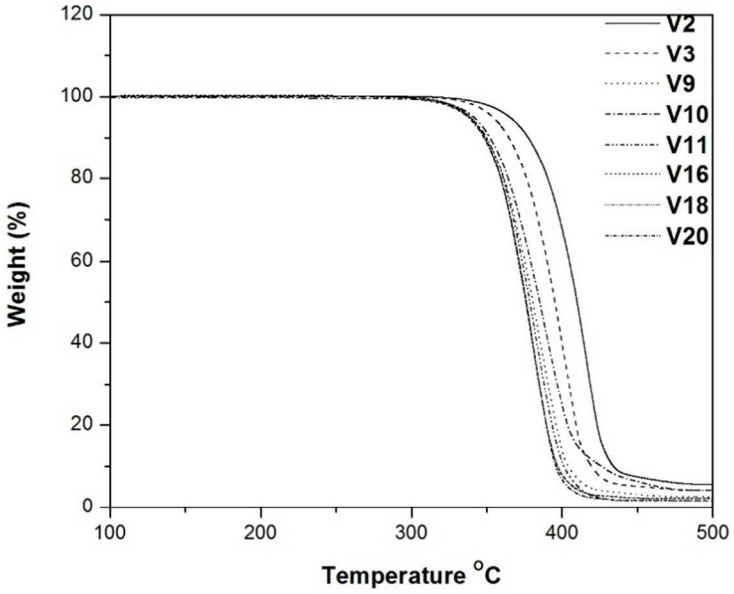

Figure 9. TGA thermograms of **V2, V3, V9, V10, V11, V16, V18** and **V20** obtained at a heating rate 10 °C/min in nitrogen.

4. Conclusions

We presented the synthesis of extended series of symmetric viologen triflimides whose chemical structures were determined by spectroscopic techniques and elemental analysis. Their thermal properties including thermotropic LC properties were examined by a number of experimental techniques that included DSC, TGA, POM and VT-XRD studies. Here, **V2** and **V3** were found to be high melting salts (> 100 °C) with high heat of enthalpies like **V1. V4** and **V5** were ionic liquids since their melting transitions were 88 and 42 °C, respectively. The lowest melting in the series was **V5. V6-V8** exhibited LC properties as well as isotropic transitions at low temperatures.[15,16] In contrast, **V9-V12** did not show any liquid-crystalline properties, although each of them had low temperature endotherm that corresponded to the crystal-crystal transition. Their high temperature endotherms corresponded to crystal-isotropic transitions at relatively high temperatures (154, 150, 166 and 199 °C, respectively). These results indicated that the longer alkyl chains of symmetric viologen structures (>8 carbon atoms) up to 12 stabilized the crystalline phase, since symmetric molecules have the best packing in the crystalline phase. In contrast, slightly asymmetric viologen structures (n = 3-11) exhibited smectic phases at low temperatures with a wide range of LC phase stability suggesting that

asymmetric caused LC phase stabilization over crystallization and those of strongly asymmetric structures exhibited low melting transitions indicative of the fact asymmetric caused a disturbance of the packing.[5] With the further increase in carbon atoms in the alkyl chain, **V14** exhibited LC properties. [17] Like **V14, V16-V20** showed thermotropic LC properties whose crystal-LC phase transitions at relatively low temperatures. They also exhibited SmA-isotropic transitions at relatively high temperatures. They showed SmC phases prior to SmA. These results suggest that the symmetric viologen structures with a large anion like triflimide require large alkyl chain lengths to form LC phases. They had excellent thermal stabilities in the temperature range of 338-365 °C. These are additional viologen salts containing triflimide counterion that exhibited thermotropic LC properties which belong to the ILCs.

Acknowledgments

We (L.S., D.M.A.-K, M.R.F, S.K.) acknowledge the support from NSF under the US Ireland R&D Partnership under Award # DMR-1410649. The work at UNLV is supported, in part, by the NSF under Grant No. 0447416 (NSF EPSCoR RING-TRUE III), NSF-SBIR Grant No. OII-0610753, NSF-STTR Grant No. IIP-0740289, and NASA GRC Contract No. NNX10CD25P. We also thank Joshua Crison for helping us in collecting the VT-XRD data of some of the salts.

References

[1] Monk PMS. The Viologens Physiochemical Properties, Synthesis and Applications of the Salts of 4,4'-Bipyridine. New York: Wiley; 1998, pp. 1-311.

[2] Hatazawa T, Terrill RH, Murray RW. Microelectrode Voltammetry and Electron Transport in an Undiluted Room Temperature Melt of an Oligo(ethylene glycol)-Tailed Viologen. Anal Chem. 1996;68:597-603.

[3] Ito-Akita K, Ohno H. Low Temperature Molten Viologens-Phase Transitions and Electrochemical Properties. Electrochem Soc Procced. 1999;99-14:193-201.

[4] Causin V, Saielli G. Effect of a structural modification of the bipyridinium core on the phase behaviour of viologen-based bistriflimide salts. J Mol Liq. 2009;145:41–47.

[5] Causin V, Saielli G. Effect of asymmetric substitution on the mesomorphic behaviour of low-melting viologen salts of bis(trifluoromethanesulfonyl)amide. J Mater Chem. 2009;19:9153–9162.

[6] Bonchio M, Carraro M, Casella G, et al. Thermal behaviour and electrochemical properties of bis(trifluoromethanesulfonyl)amide and dodecatungstosilicate viologen dimers. Phys Chem Chem Phys. 2012;14:2710– 2717.

[7] Gunaratne HQN, Nockemann P, Olejarz S, Reid SM, Seddon KR, Srinivasan G. Ionic Liquids with Solvatochromic and Charge-Transfer Functionalities Incorporating the Viologen Moiety. Aust J Chem. 2013;66:607-611.

[8] Jordão N, Cabrita L, Pina F, Branco LC. Novel Bipyridinium Ionic Liquids as Liquid Electrochromic Devices. Chem Eur J. 2014;20:3982-3988.

[9] Tahara H, Furue Y, Suenaga C, Sagara T. A Dialkyl Viologen Ionic Liquid: X-ray Crystal Structure Analysis of Bis(trifluoromethanesulfonyl)imide Salts. Cryst Growth Des. 2015;15:4735-4740.

[10] Jordão N, Cruz H, Branco A, Pina F, Branco LC. Electrochromic Devices Based on Disubstituted Oxo-Bipyridinium Ionic Liquids. ChemPhysChem. 2015;80:202-208.

[11] Yu LP, Samulski ET. Ionomeric Liquid Crystals. In: Griffin AC, Johnson JF, editors. Oriented Fluids and Liquid Crystals. Vol. 4. New York: Plenum; 1984, p. 697-704.

[12] Tabushi I, Yamamura K, Kominami K. Electric Stimulus-Response Behavior of Liquid-Crystalline Viologen. J. Am. Chem. Soc. 1986;108:6409-6410.
[13] Yamamura K, Okada Y, Ono S, Kominami K, Tabushi I. New Liquid Crystalline Viologens Exhibiting Electric Stimulus-Response Behavior. Tetrahedron Lett. 1987;28:6475-6478.
[14] Haramoto Y, Yin M, Matukawa Y, Ujiie S, Nanasawa M. A new ionic liquid crystal compound with viologen group in the principal structure. Liq Cryst. 1995;19:319-320.
[15] Bhowmik PK, Han H, Cebe JJ, et al. Ambient temperature thermotropic liquid crystalline viologen bis(triflimide) salts. Liq Cryst. 2003;30:1433–1440.
[16] Bhowmik PK, Han H, Nedeltchev IK, Cebe JJ. Room-Temperature Thermotropic Ionic Liquid Crystals: Viologen Bis(triflimide) Salts. Mol Cryst Liq Cryst. 2004;419:27-46.
[17] Casella G, Causin V, Rastrelli F, et al. Viologen-based ionic liquid crystals: induction of a smectic A phase by dimerisation. Phys Chem Chem Phys. 2014;16:5048– 5051.
[18] Casella G, Causin V, Rastrelli F, Giacomo Saielli G. Ionic liquid crystals based on viologen dimers: tuning the mesomorphism by varying the conformational freedom of the ionic layer. Liq Cryst. 2016;43:1161-1173.
[19] Binnemans K. Ionic Liquid Crystals. Chem Rev. 2005;105:4148-4204.
[20] Axenov K, Laschat S. Thermotropic ionic liquid crystals. Materials. 2011;4:206-259.
[21] Causin V, Saielli G. Ionic liquid crystals. In: Mohammad A, Inamuddin D, editors. Green solvents II. Properties and applications of ionic liquids. UK: Springer; 2012. p. 79–118
[22] Mansueto M, Laschat S. Ionic Liquid Crystals. In: Goodby JW, Collings PJ, Kato T, Tschierske C, Gleeson H, Raynes P, editors. Handbook of Liquid Crystals. Vol. 6: Nanostructured and Amphiphilic Liquid Crystals, 2nd ed. Weinheim: Wiley-VCH; 2014; p. 231−280.
[23] Fernandez AA, Kouwer PH. Key Developments in Ionic Liquid Crystals. Int J Mol Sci. 2016;17:731; doi:10.3390/ijms17050731
[24] Goossens K, Lava K, Bielawski CW, Binnemans K. Ionic Liquid Crystals: Versatile Materials. Chem Rev. 2016;116:4643-4807.
[25] Wasserscheid P, Welton T. Ionic Liquids in Synthesis. 2nd ed. Weinheim: Wiley-VCH; 2007.
[26] C. Weber CC, Mastersa AF, Maschmeyer T. Structural features of ionic liquids: consequences for material preparation and organic reactivity. Green Chem. 2013;15:2655-2679.
[27] Nelyubina YV, Shaplov AS, Lozinskaya EI, Buzin MI, Vygodskii YS. A New Volume-Based Approach for Predicting Thermophysical Behavior of Ionic Liquids and Ionic Liquid Crystals. J Am Chem Soc. 2016;138:10076-10079.
[28] Goossens K, Lava K, Nockemann P, Van Hecke K, Van Meervelt L, Pattison P, Binnemans K, Cardinaels T. Pyrrolidinium Ionic Liquid Crystals with Pendant Mesogenic Groups. Langmuir. 2009; 25:5881-5897.
[29] Douce L, Suisse J-M, Guillon D, Taubert A. Imidazolium-based liquid crystals: a modular platform for versatile new materials with finely tuneable properties and behavior. Liq Cryst. 2011; 38: 1653-1661.
[30] Schenkel MR, Shao R, Robertson LA, et al. New ionic organic compounds containing a linear tris(imidazolium) core and their thermotropic liquid crystal behaviour. Liq Cryst. 2013;40:1067–1081.
[31] Schenkel MR, Hooper JB, Moran MJ, et al. Effect of counter-ion on the thermotropic liquid crystal behaviour of bis(alkyl)-tris(imidazolium salt) compounds. Liq Cryst. 2014;41:1668–

1685.
[32] Li T, Xu F, Shi W. Ionic liquid crystals based on 1-alkyl-3-methylimidazolium cations and perfluorinated sulfonylimide anions. Chem Phys Lett. 2015;628:9-15.
[33] Timko L, Fischer-Fodor E, Garajová M, Mrva M, Chereches G, Ondriska F, Bukovský M, Lukáč M, Karlovská J, Kubincová J, Devínsky F. Synthesis of structural analogues of hexadecylphosphocholine and their antineoplastic, antimicrobial and amoebicidal activity. Eur J Med Chem. 2015;93:263-273.
[34] Johns WF, Lukes RM, Sarett LH. Approaches to the Total Synthesis of Adrenal Steroids. X. A New Method for the Attachment of Ring D. Part D. J Am Chem Soc. 1954;76:5026-5030.
[35] Gray GW, Goodby JWG. Smectic Liquid Crystals: Textures and Structures, Glasgow: Leonard Hill; 1984.
[36] Collins PJ, Hird M. Introduction to Liquid Crystals Chemistry and Physics, Bristol, PA: Taylor & Francis; 1997.
[38] Demus D, Goodby JW, Gray GW, Spiess H.-W, Vill V. editors. Handbook of Liquid Crystals vols. 1-3. Weinheim: Wiley-VCH; 1998.
[39] Dierking I. Textures of Liquid Crystals, Weinheim: Wiley-VCH; 2003.
[40] Hanwell MD, Curtis DE, Lonie DC, Vandermeersch T, Zurek E, Hutchison GR. Avogadro: An advanced semantic chemical editor, visualization, and analysis platform. J Cheminform. 2012; 4: 17.
[41] Wasserscheid P. Volatile times for ionic liquids. Nature. 2006;439:797.
[42] Earle MJ, Esperança JMSS, Gilea MA, Lopes JNC, Rebelo LPN, Magee JW, Seddon KR, Widegren JA. The distillation and volatility of ionic liquids. Nature. 2006;439:831-834.
[43] Widegren JA, Wang Y-M, Henderson WA, Magee JW. Relative Volatilities of Ionic Liquids by Vacuum Distillation of Mixtures. J Phys Chem B. 2007;111:8959-8964.
[44] Esperança JMSS, Lopes JNC, Tariq M, Santos LMNBF, Magee JW, Rebelo, LPN. Volatility of Aprotic Ionic Liquids-Review. J Chem Eng Data. 2010;55:3-12.
[45] Nedeltchev AK, Han H, Bhowmik PK. Design and synthesis of photoactive ionic amorphous materials. J Mater Chem. 2011;21:12717-12724.
[46] Jo TS, Nedeltchev AK, Biswas B. et al. Synthesis and characterization of poly(pyridinium salts) derived from various aromatic diamines. Polymer (Guildf). 2012;53:1063-1071.
[47] Jo TS, Koh JJ, Han H, Bhowmik PK. Solution, thermal and optical properties of bis(pyridinium salt)s as ionic liquids. Mater Chem Phys. 2013;139:901-910.

Supplementary Information

Thermotropic Liquid-Crystalline Properties of Extended Viologen Bis(triflimide) Salts

Pradip K. Bhowmik,[a] Shane T. Killarney,[a] Jessa Rose A. Li,[a] Jung Jae Koh,[a] and Haesook Han[a]
[a]Department of Chemistry and Biochemistry, University of Nevada Las Vegas, 4505 S. Maryland Parkway, Box 454003, Las Vegas, NV 89154, USA
E-mail:pradip.bhowmik@unlv.edu
Lewis Sharpnack[b] Deña M. Agra-Kooijman,[b] Michael R. Fisch,[c] and Satyendra Kumar[d]
[b]Department of Physics and [c]College of Applied Engineering, Sustainability and Technology, Kent State University, Kent, OH 44242, USA
[d]Division of Research, University at Albany, Albany, NY 12222, USA

List of Contents

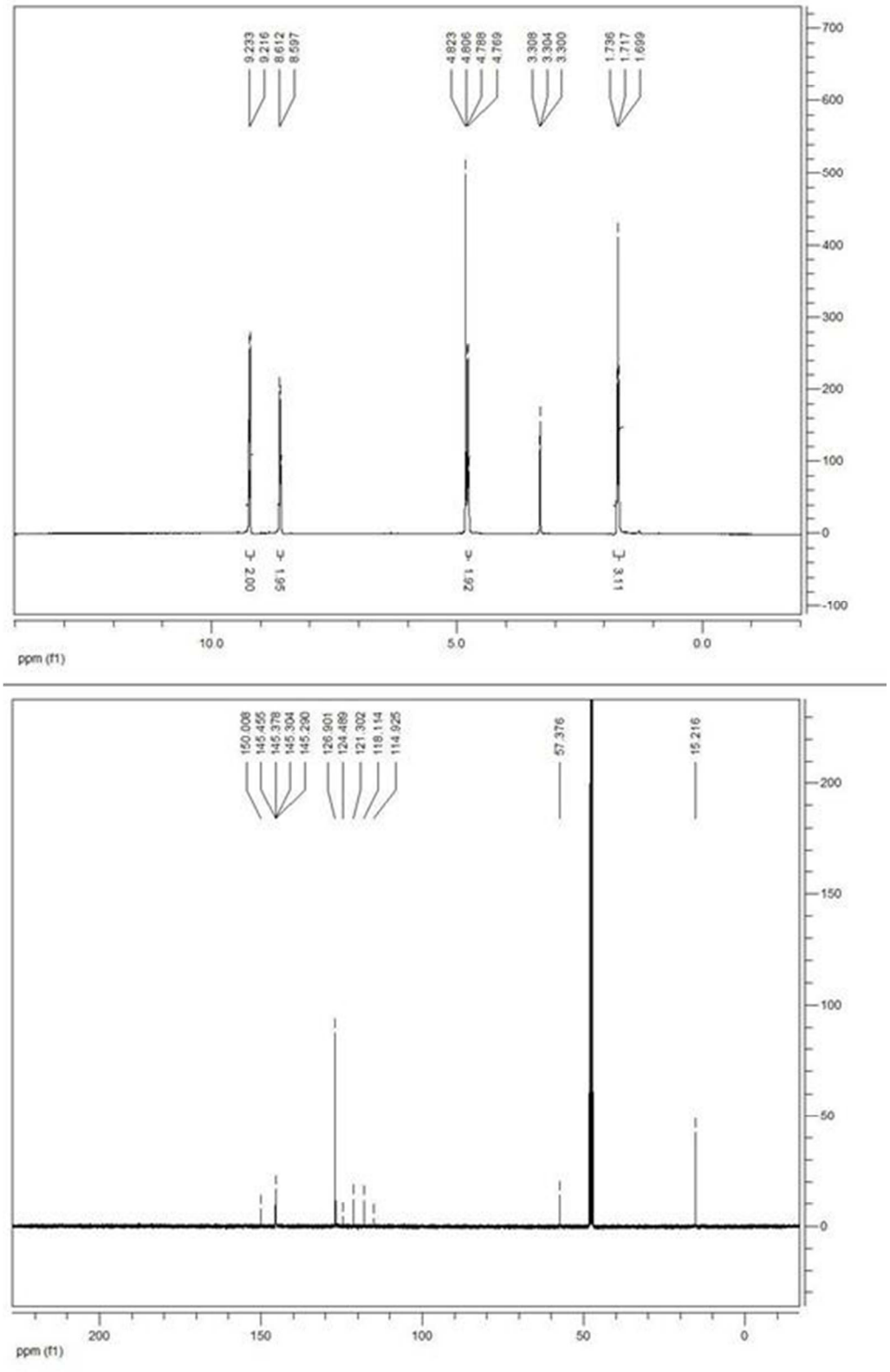

Figure S1. ^{1}H and ^{13}C NMR spectra of **V2** in CD_3OD recorded at room temperature.

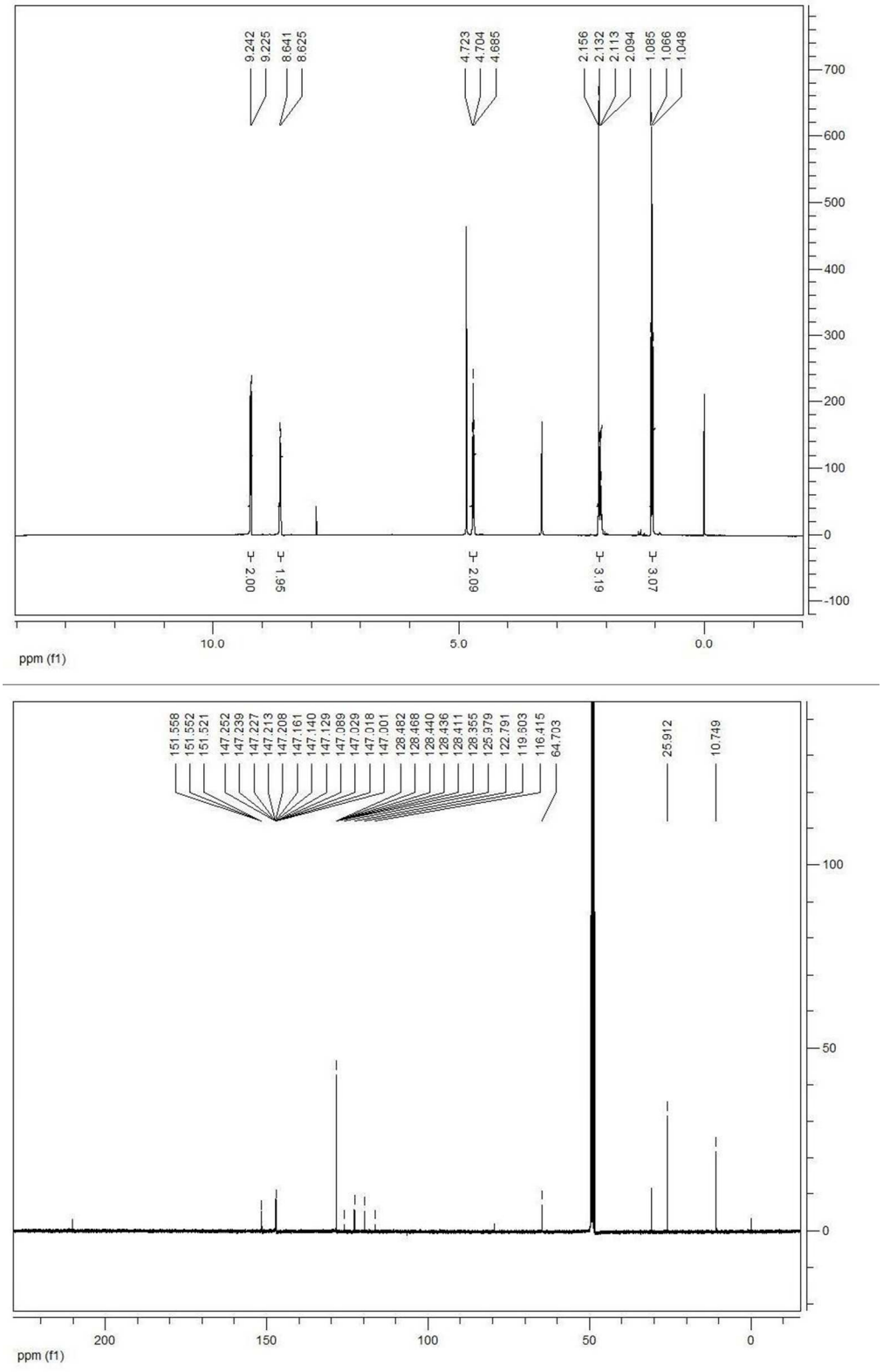

Figure S2. ^{1}H and ^{13}C NMR spectra of **V3** in CD_3OD recorded at room temperature.

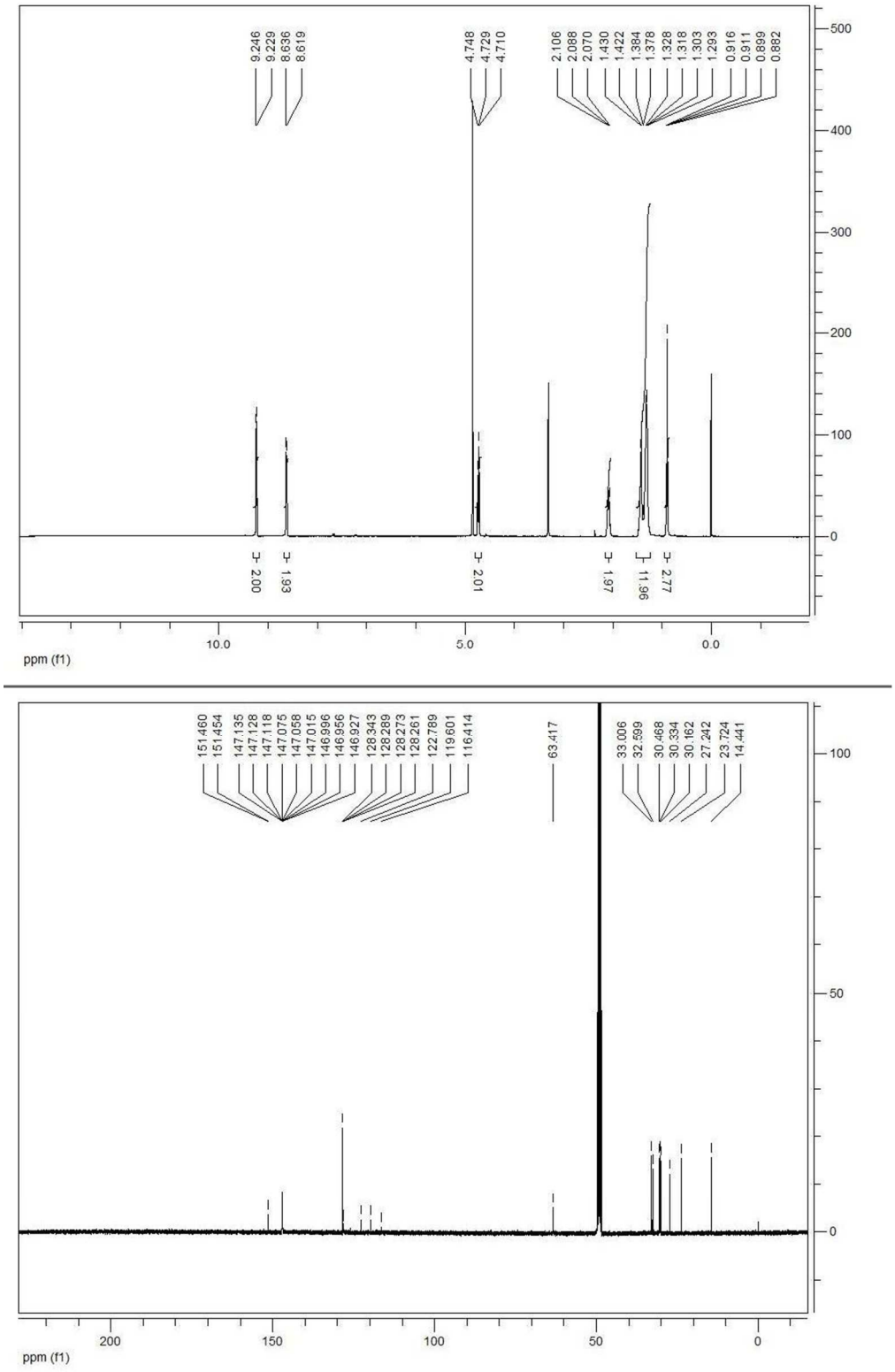

Figure S3. ^{1}H and ^{13}C NMR spectra of **V9** in CD_3OD recorded at room temperature.

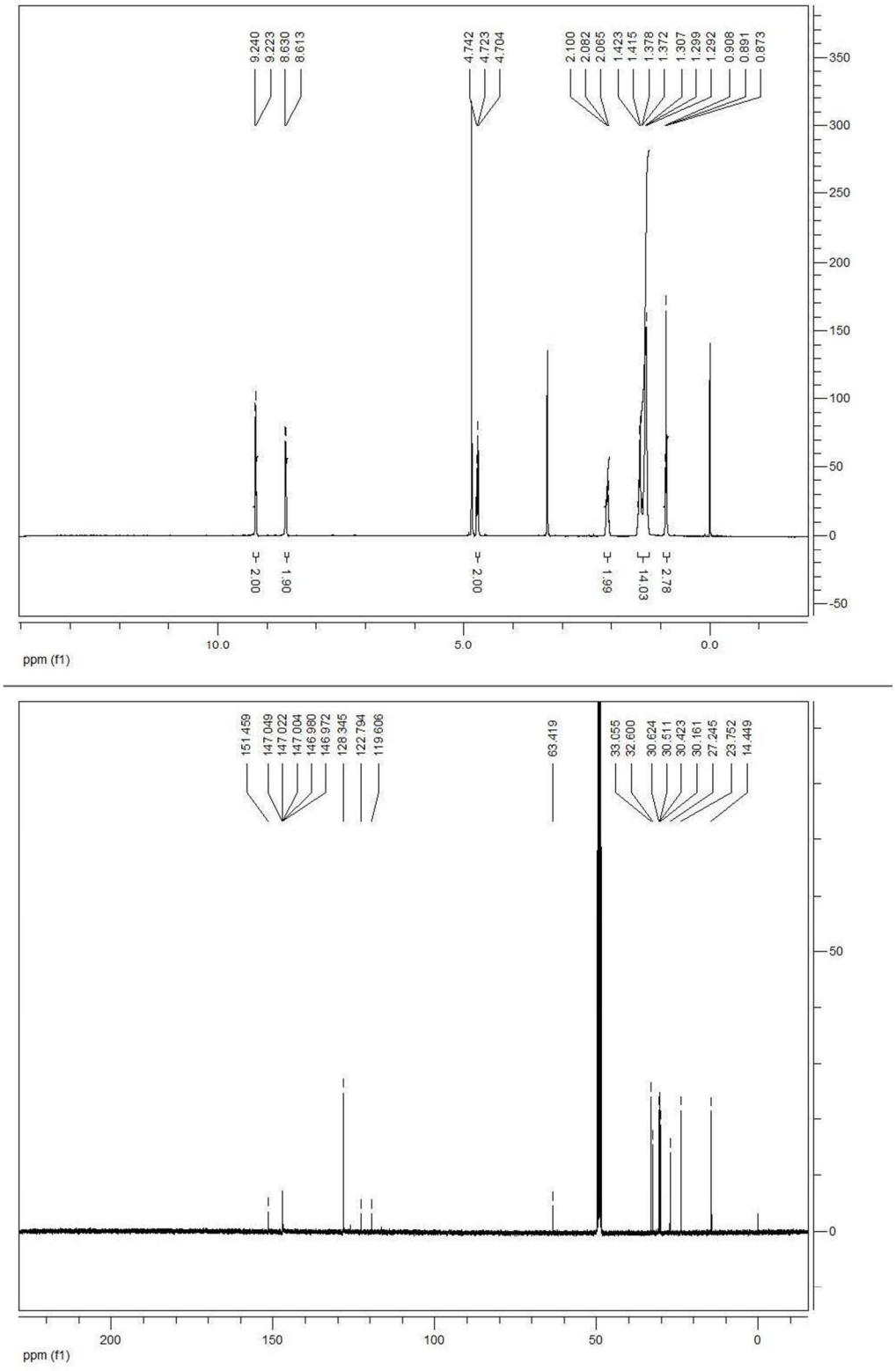

Figure S4. ^{1}H and ^{13}C NMR spectra of **V10** in CD_3OD recorded at room temperature.

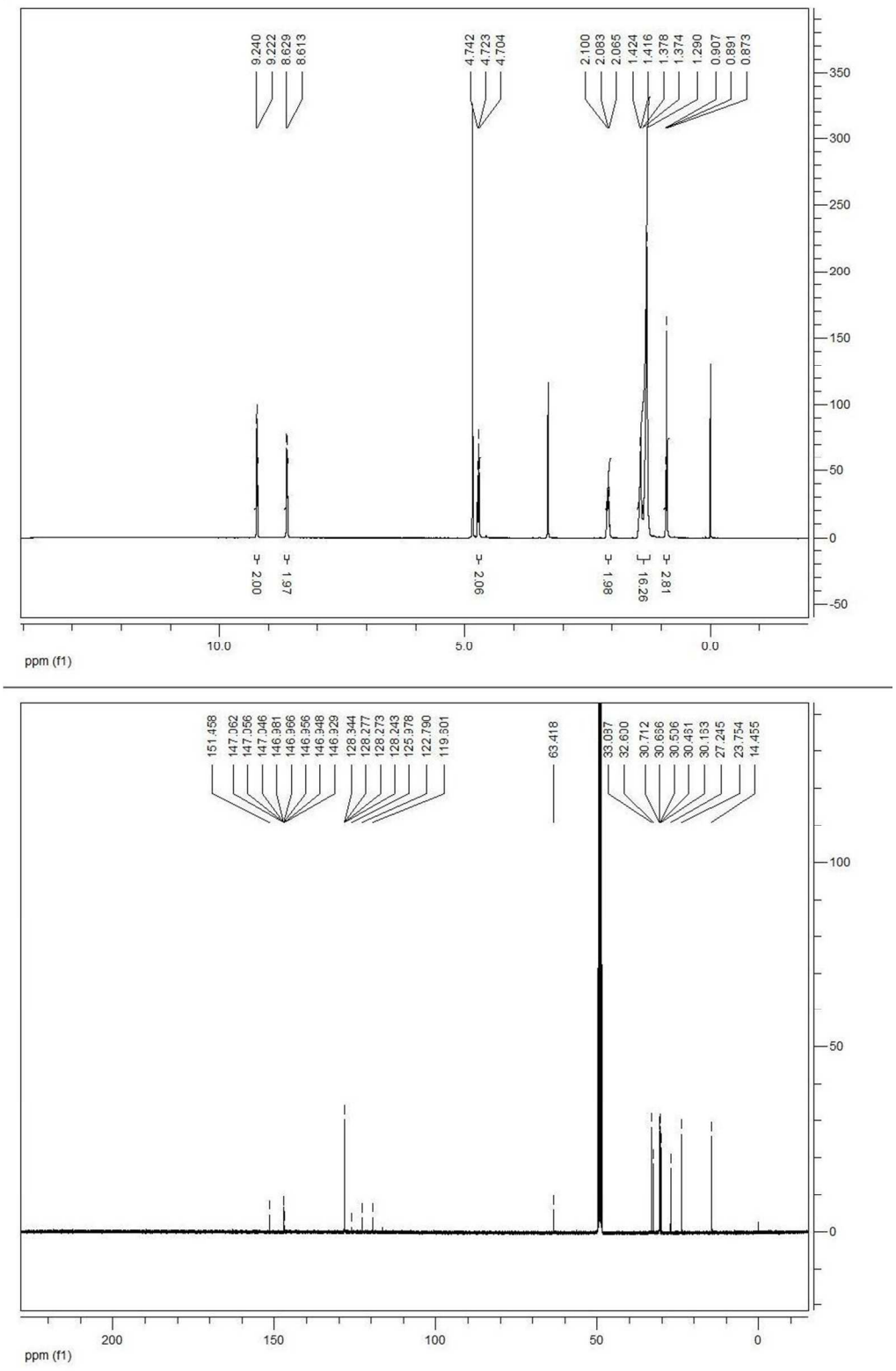

Figure S5. ^{1}H and ^{13}C NMR spectra of **V11** in CD_3OD recorded at room temperature.

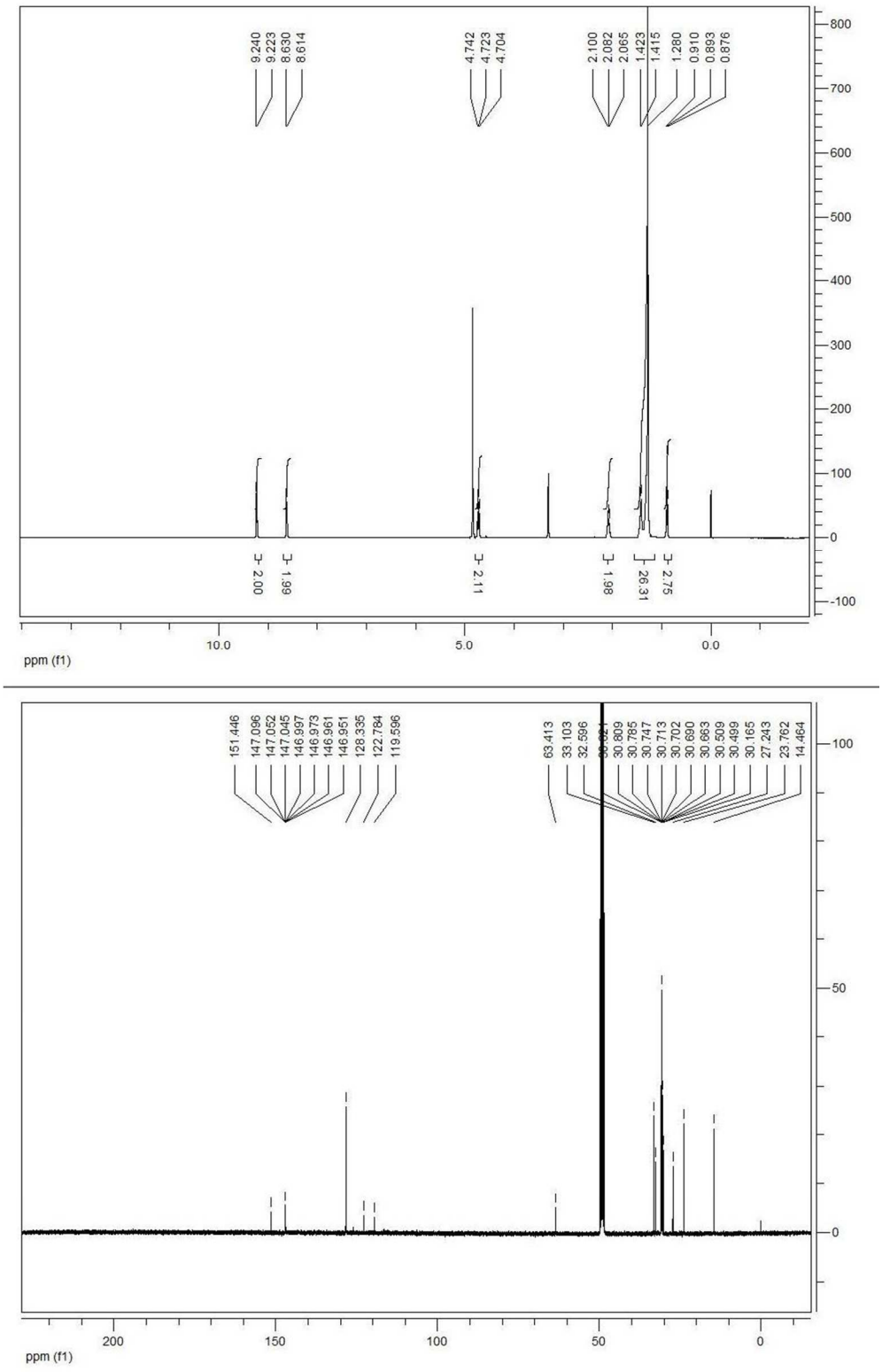

Figure S6. ^{1}H and ^{13}C NMR spectra of **V16** in CD_3OD recorded at room temperature.

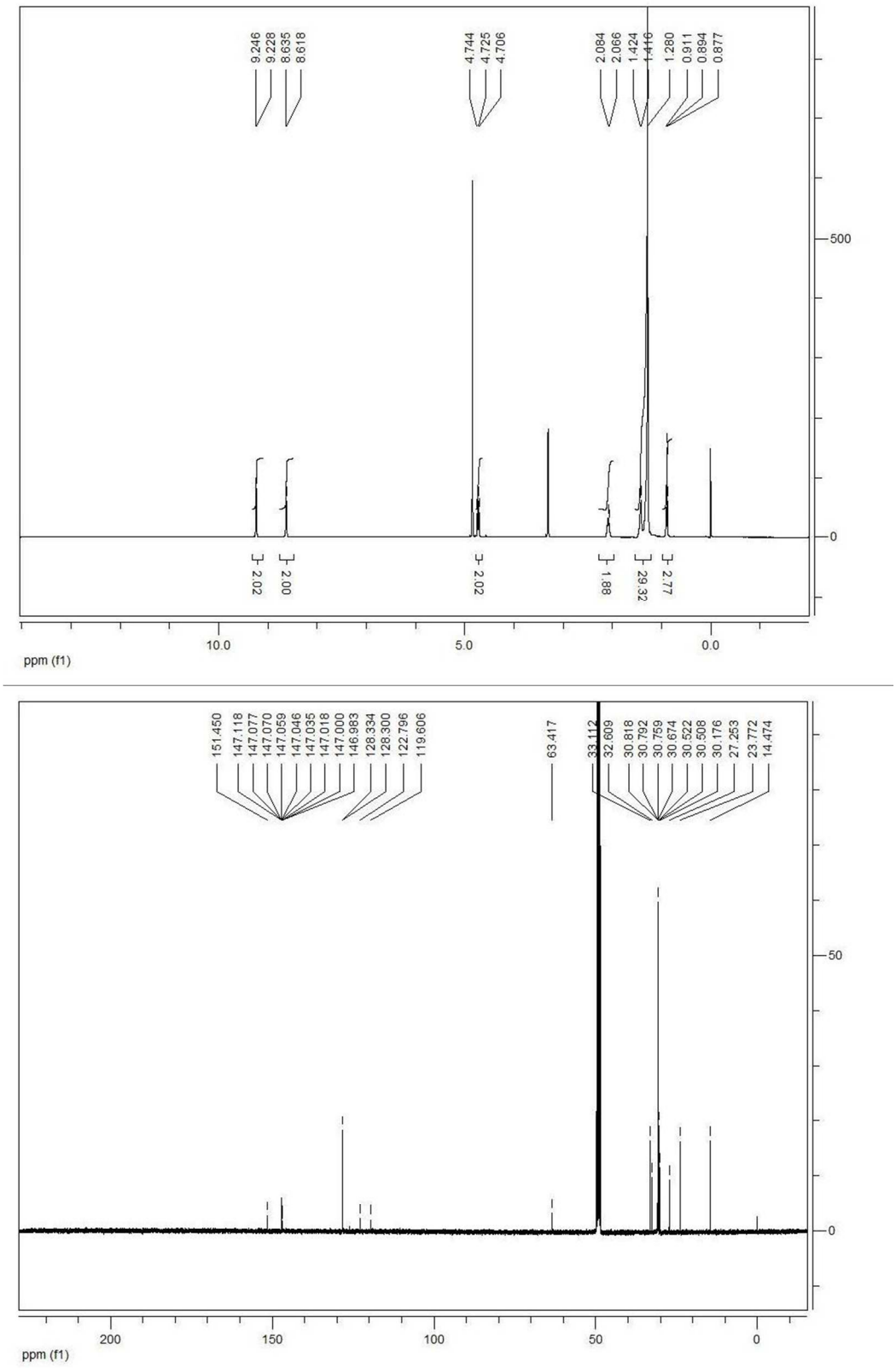

Figure S7. ^{1}H and ^{13}C NMR spectra of **V18** in CD_3OD recorded at room temperature.

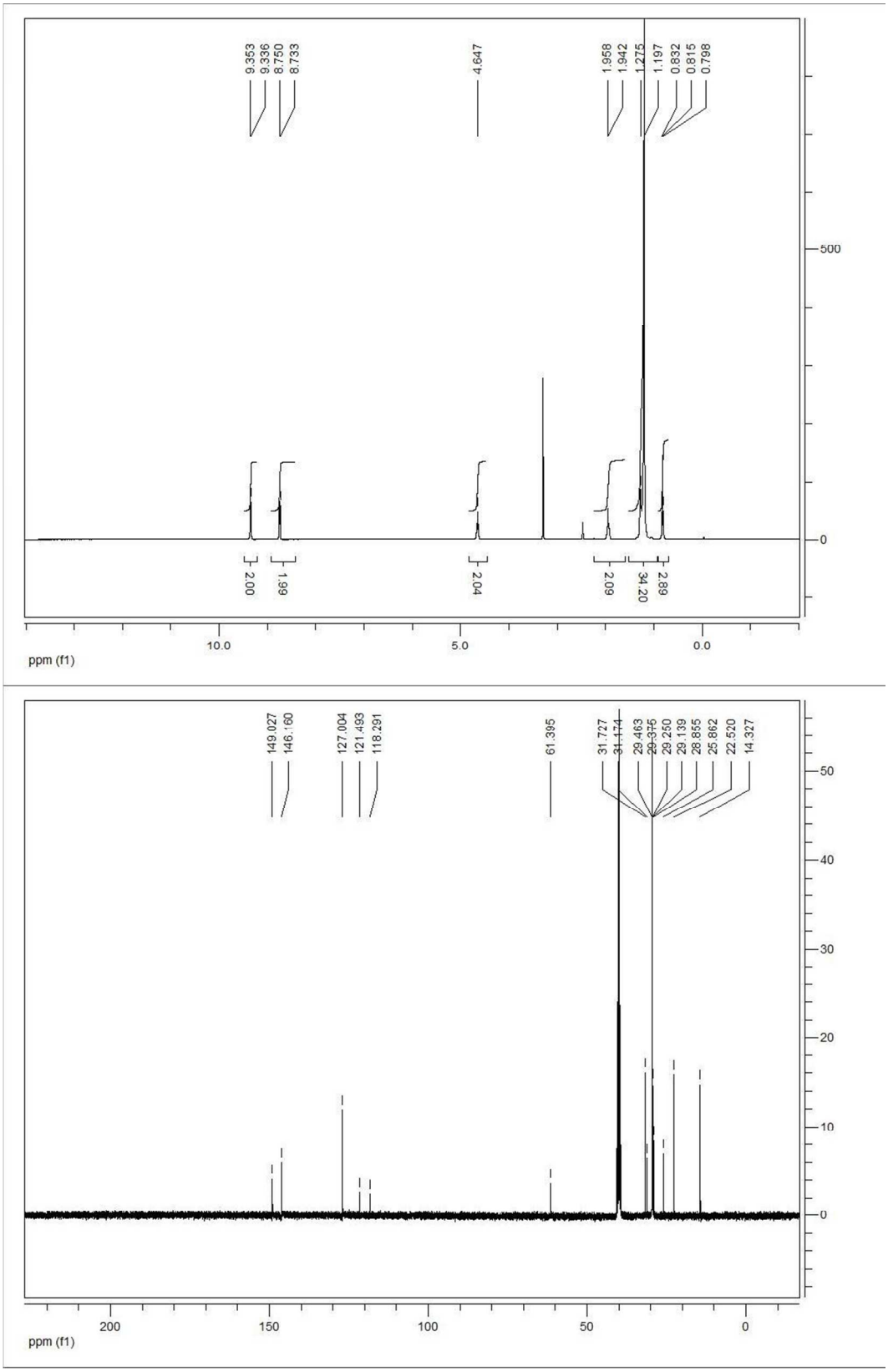

Figure S8. ^{1}H and ^{13}C NMR spectra of **V20** in CD_3OD recorded at room temperature.

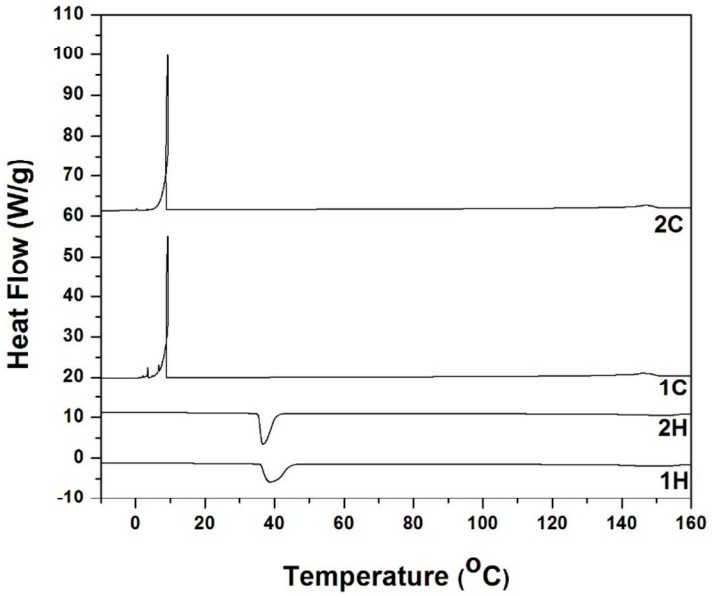

Figure S9. DSC thermograms of **V9** obtained at heating and cooling rates of 10 °C/min in nitrogen.

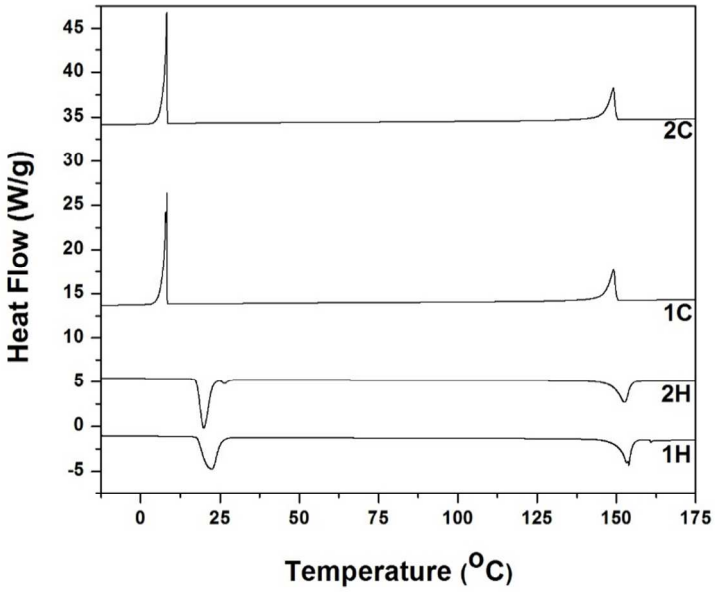

Figure S10. DSC thermograms of **V10** obtained at heating and cooling rates of 10 °C/min in nitrogen.

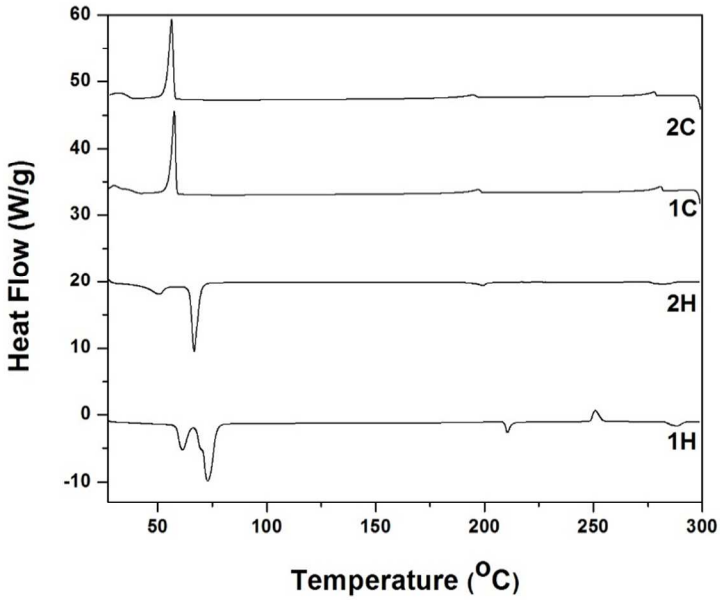

Figure S11. DSC thermograms of **V20** obtained at heating and cooling rates of 10 °C/min in nitrogen.